

STRATIGRAPHIC RECORD OF PLIOCENE-PLEISTOCENE BASIN EVOLUTION  
AND DEFORMATION ALONG THE SAN ANDREAS FAULT, MECCA HILLS,  
CALIFORNIA

by

JAMES CARLTON MCNABB

A THESIS

Presented to the Department of Geological Sciences  
and the Graduate School of the University of Oregon  
in partial fulfillment of the requirements  
for the degree of  
Master of Science

December 2013

THESIS APPROVAL PAGE

Student: James Carlton McNabb

Title: Stratigraphic Record of Pliocene-Pleistocene Basin Evolution and Deformation  
Along the San Andreas Fault, Mecca Hills, California

This thesis has been accepted and approved in partial fulfillment of the requirements for  
the Master of Science degree in the Department of Geological Sciences by:

Dr. Rebecca J. Dorsey	Chairperson
Dr. Ray J. Weldon II	Member
Dr. Josh J. Roering	Member

and

Kimberly Andrews Espy	Vice President for Research and Innovation; Dean of the Graduate School
-----------------------	--

Original approval signatures are on file with the University of Oregon Graduate School.

Degree awarded December 2013

© 2013 James Carlton McNabb

## THESIS ABSTRACT

James Carlton McNabb

Master of Science

Department of Geological Sciences

December 2013

Title: Stratigraphic Record of Pliocene-Pleistocene Basin Evolution and Deformation  
Along the San Andreas Fault, Mecca Hills, California

Sedimentary rocks in the Mecca Hills record a 3-4 Myr history of basin evolution and deformation within the southern San Andreas fault (SAF) zone. Detailed geologic mapping, measured sections, lithofacies analysis, and preliminary paleomagnetic data indicate that sedimentation and deformation in the Mecca Hills resulted from evolution of local fault zone complexities superimposed on regional subsidence and uplift. Sediment was derived from sources northeast of the SAF and transported southeast along the fault zone in large rivers, alluvial fans, and a smaller fault-bounded lake. Inversion of the Painted Canyon fault from oblique SW-side down to SW-side up slip was the main control on local deposition and deformation. Regional controls are suggested by an angular unconformity observed in the Mecca and Indio Hills along ~50 km of the SAF, and synchronous post-740 ka uplift northeast of the SAF along ~80 km of the fault zone.

This thesis includes the “Geologic Map of the Central Mecca Hills, Southern California” as supplemental material.

## CURRICULUM VITAE

NAME OF AUTHOR: James Carlton McNabb

### GRADUATE AND UNDERGRADUATE SCHOOLS ATTENDED:

University of Oregon, Eugene  
University of Arizona, Tucson

### DEGREES AWARDED:

Master of Science, Sedimentology and Tectonics, 2013, University of Oregon  
Bachelor of Science, Geology, 2010, University of Arizona

### AREAS OF SPECIAL INTEREST:

Sedimentology  
Structural geology  
Tectonics  
Geologic mapping  
Geochronology

### PROFESSIONAL EXPERIENCE:

Lab Assistant, University of Arizona LaserChron Center, 6 mos.

Graduate Teaching Fellow, University of Oregon, 2011 to present

### GRANTS, AWARDS, AND HONORS:

Graduate Student Research Grant, Geological Society of America, 2012

### PUBLICATIONS:

DeCelles, P. G., B. Carrapa, B.K. Horton, J. McNabb, J. Boyd, 2011, Cordilleran Hinterland Basins as Recorders of Lithospheric Removal in the Central Andes, Abstract T13I-06 presented at American Geophysical Union, Fall Meeting 2011 San Francisco, Calif., Dec. 3-7.

DeCelles, P.G., Carrapa, B., Horton, B.K., McNabb, J., Gehrels, G.E., Boyd, J., 2013 (in press) Arizaro basin, central Andean hinterland: response to partial lithosphere removal? In DeCelles, P.G., Ducea, M.N., Carrapa, B., and Kapp, P., eds., *Geodynamics of a Cordilleran Orogenic System: The Central Andes of Argentina and Northern Chile*, Geological Society of American Memoir.

Dorsey, R.J., V.E. Langenheim, J.C. McNabb, 2012, Geometry, Timing, and Rates of Active Northeast Tilting Across the Southern Coachella Valley and Santa Rosa Mountains, Abstract T51B-2568 presented at 2012 Fall Meeting, AGU, San Francisco, Calif., Dec. 3-7.

Housen, B.A., L. Fattaruso, J.C. McNabb, R.J. Dorsey, G.T. Messe, M.L. Cooke, 2013, Magnetostratigraphy and Paleomagnetism of the Palm Spring and Mecca Formations, Mecca Hills, CA: spatial variation of vertical axis rotation in the Coachella Valley, Abstract T11D-2485 presented at 2013 Fall Meeting, AGU, San Francisco, Calif., Dec 9-14.

McNabb, J.C., R.J. Dorsey, 2012, Stratigraphic Record of Vertical Crustal Motions in the Past 2-3 Ma Along the Southern San Andreas Fault, Mecca Hills, California, Abstract T51B-2582 presented at 2012 Fall Meeting, AGU, San Francisco, Calif., Dec. 3-7.

McNabb, J.C., R.J. Dorsey; B.A. Housen, G.T. Messe, 2013, Stratigraphic Record of Basin Formation, Deformation, and Destruction in the Past 2 Ma Along the Southern San Andreas Fault, Mecca Hills, California, Abstract T11D-2484 presented at 2013 Fall Meeting, AGU, San Francisco, Calif., Dec 9-14.

Messe, G.T., J.C. McNabb, B.A. Housen, R.J. Dorsey, 2012, Magnetostratigraphy of the Palm Spring Formation, Mecca Hills, CA, *GSA Abstracts with Programs*, 44, xxx.

Messe, G.T. B.A. Housen, R. F. Burmester, J.C. McNabb, R.J. Dorsey, 2013, Magnetostratigraphy and Paleocurrent Directions for the Upper Member of the Palm Spring Formation, Mecca Hills, CA, Abstract GP41A-1108 presented at 2013 Fall Meeting, AGU, San Francisco, Calif., Dec 9-14.

## ACKNOWLEDGMENTS

First and foremost I wish to express my immense gratitude for Dr. Rebecca Dorsey who has given me the opportunity to grow and evolve as a geoscientist with her unwavering guidance and enthusiasm. She has instilled in me great tenacity and humility that go beyond my academic pursuits. I owe special thanks to Dr. Ray Weldon, Dr. Josh Roering, and Michael Rymer for offering their guidance. Also thanks to Dr. Bernard Housen and Graham Messe for their hard work both in the field and in the paleomagnetic laboratory, and Michele Cooke and Laura Fattarusso for their unique perspectives in regards to the Mecca Hills. This research benefitted from many thoughtful discussions with Ashley Streig and Lauren Austin. Lastly, thanks to my field assistant, Jacob Staff, who never questioned my sanity even after a lengthy ~140 field days.

This study would not have been possible without the love and support of my family. They inspire me everyday to continue to pursue my passions with unwavering support. I would especially like to express my love and gratitude for my sister Amy, who reminds me everyday to love unconditionally. I look forward to taking you to Disneyland.

This research was supported in part by a grant from the National Science Foundation (EAR-1144946) to Dr. Rebecca J. Dorsey at the University of Oregon, and by a Graduate Student research Grant from the Geological Society of America.

## TABLE OF CONTENTS

Chapter	Page
I. INTRODUCTION .....	1
II. GEOLOGIC SETTING .....	3
Southern San Andreas Fault Zone.....	3
Mecca Hills.....	5
III. METHODS.....	12
Geologic Mapping.....	12
Measured Stratigraphic Sections .....	12
Paleocurrents & Clast Counts.....	13
Paleomagnetic Analysis .....	13
III. RESULTS .....	16
Geologic Map and Cross Sections.....	16
Sedimentary Lithofacies.....	19
Mecca Conglomerate (Pm).....	19
Palm Spring Formation .....	23
Lower Member, Palm Spring Formation (Qpl).....	23
Upper Member, Palm Spring Formation (Qpu) .....	25
Ocotillo Conglomerate (Qo).....	29
Stratigraphic and Basinal Architecture.....	30
Lacustrine Sequence, Upper Member Palm Spring Formation.....	30
Upper Member Northeast of the Painted Canyon Fault .....	32
Progressive Unconformity Southwest of the Painted Canyon Fault .....	34

Chapter	Page
Stratigraphic Ages and Sediment-Accumulation Rates .....	36
Measured Section 1 .....	36
Measured Section 3 .....	37
V. DISCUSSION.....	41
Paleogeographic and Fault Reconstructions.....	41
Mecca Conglomerate.....	41
Lower Member, Palm Spring Formation .....	44
Deformation, Erosion, Angular Unconformity .....	44
Upper Member, Palm Spring Formation.....	45
Ocotillo Conglomerate (ca. 0.76 Ma).....	46
Local Versus Regional Scale of Fault-Zone Evolution.....	46
VI. CONCLUSIONS.....	50
REFERENCES CITED .....	52
SUPPLEMENTAL FILES	
GEOLOGIC MAP OF THE CENTRAL MECCA HILLS, SOUTHERN CALIFORNIA (1:15,000)	

## LIST OF FIGURES

Figure	Page
1. Geologic map of the Coachella. Modified from map compiled by Dorsey, 2011 (unpub.). Abbreviations: BF, Banning fault; BSZ, Brawley seismic zone; DH, Durmid Hill; EFZ, Extra fault zone; IH, Indio Hills; MCF, Mission Creek fault; MH, Mecca Hills; PMF, Pinto Mtn. fault.....	4
2. Geologic map of the Mecca Hills. Modified from map compiled by Dorsey, (2011, unpub.). Inset map shows structural blocks from Sylvester and Smith (1927). Abbreviations: SAF, San Andreas Fault; SCF, Skeleton Canyon Fault; PCF, Painted Canyon Fault; PF.....	6
3. Simplified diagram of stratigraphic and basement relationships southwest and northeast of the Painted Canyon Fault near Painted Canyon .....	7
4. Geologic map of the Mecca Hills near Painted Canyon (this study). Abbreviations: SAF, San Andreas fault; SCF, Skeleton Canyon fault; PCF, Painted Canyon fault; PF, Platform fault; ECF, Eagle Canyon fault .....	8
5. Geologic cross section from lines A-A' and B-B' in Figure 4. Abbreviations: SAF, San Andreas fault; SCF, Skeleton Canyon Fault; PCF, Painted Canyon fault; PF, Platform fault; ECF, Eagle Canyon fault .....	11
6. (A) Measured stratigraphic Section 1, northeast of the Painted Canyon Fault with our preferred correlations to the Geomagnetic Polarity Time Scale (GPTS), and estimated ages for limestone LM and the angular unconformity. (B) Measured stratigraphic Section 3 .....	17
7. Photographs of sedimentary rocks exposed in the Mecca Hills. A) Mecca Conglomerate in lower Painted Canyon. Hammer circled for scale. (B) Fining upward sequence from pebbly sandstone to siltstone in the lower member of the Palm Spring Formation. Hammer circled for scale .....	22
8. Photographs of stratigraphic relationships in the Mecca Hills. (A) Coarsening upward sequences in lacustrine and nearshore deposits capped by lacustrine flooding surfaces between Eagle Canyon and the PCF. (B) Medial alluvial fan deposits (Qpu-pss) capped by lacustrine .....	24
9. Facies panel for Section 1 showing northwest transgression of lacustrine mudstone and siltstone (Qpums) and nearshore sandstone and siltstone (Qpubss) over distal alluvial fan pebbly sandstone (Qpups) though time. Marker horizons shown as pink lines; LM is limestone marker horizon.....	31

Figure	Page
10. Geologic cross section line C – C’ in Figure 4 on the northeast side of the PCF. Marker horizons used to correlate measured section 1 shown as pink lines and labeled (e.g. M2). LM is limestone marker horizon. Stars are calculated depth to basement projected into section from nearby basement.....	33
11. Map showing two angular unconformities (red lines), one in the northwest and one in the southeast, that separate the lower and upper members of the Palm Spring Formation. Both map into laterally equivalent conformable surfaces (yellow lines). Between the unconformities.....	35
12. Simplified diagram illustrating the stratigraphic relationships in Figure 11 from northwest to southeast across Painted Canyon. Prominent lower unconformity in the southeast maps into a laterally equivalent conformable surface in the northwest. Upper unconformity in northwest maps .....	36
13. Paleogeographic reconstructions of the Mecca Hills from ~3.5 – 0.74 Ma. (A) Initiation of southwest-side down slip on the PCF and deposition of the Mecca Conglomerate between ~3.0-4.8Ma (B) Between 2.6 and 3.7 Ma the southeast-directed fluvial system deposited the lower member .....	42
14. Block diagrams illustrating the evolution of vertical crustal motions and depositional systems from ~3.5 – 1 Ma in the Mecca Hills. (A) Southwest-side down slip on the PCF and deposition of the Mecca Conglomerate. (B) Overlapping deposition of the regionally extensive facies .....	43

LIST OF TABLES

Table	Page
1. (A) Descriptions and interpretations of sedimentary rock facies .....	20
2. Calculated sediment-accumulation rates based on magnetic reversal ages and stratigraphic thickness from Section 1 .....	38

# CHAPTER I

## INTRODUCTION

Subsidence and uplift of sedimentary basins is widely observed along continental transform faults (e.g., Crowell, 1974; Christie-Blick and Biddle, 1985; Weldon et al., 1993; Sadler et al., 1993; Aksu et al., 2000; Seeber et al., 2006, 2010), yet the controls on the evolution of these basins through time remain incompletely understood. Models that predict transpression and transtension due to relative plate-motion obliquity along strike-slip faults have failed to describe observed patterns of uplift and subsidence along the San Andreas Fault (SAF) (e.g., Spotila et al., 2007a, b), suggesting the influence of additional factors such as structural complexity, rock strength, crustal anisotropy, local changes in relative block motions, or regional changes in tectonic kinematics. Sedimentary rocks deposited and subsequently uplifted along strike-slip faults record the basinal response to evolving fault complexities, and thus offer unique insights into the 4-D evolution of strain in these settings.

The Mecca Hills on the northeast side of Coachella Valley, southern California, preserve > 1.3 km of superbly exposed Pliocene-Pleistocene terrestrial sedimentary rocks along the southern San Andreas fault and associated strike-slip faults. Recent uplift and erosion in the Mecca Hills allows for detailed sedimentological and stratigraphic analysis through nearly continuous stratigraphic sections, making it an excellent natural laboratory to study the stratigraphic record of strike-slip fault-related deformation.

Previous workers have documented the stratigraphy and modern structure of the Mecca Hills (summarized below), but until this study the evolution of depositional

systems in response to changing vertical crustal motions through time was not well understood. This study combines geologic mapping, stratigraphic analysis, new magnetostratigraphic data, and determination of sedimentary provenance to reconstruct past landscapes and environments in response to crustal deformation. This allows us to interpret a 3 - 4 Myr history of strike-slip related basin formation in the Mecca Hills, and assess the underlying controls on vertical crustal motions within this part of the southern San Andreas fault zone.

## CHAPTER II

### GEOLOGIC SETTING

#### **Southern San Andreas Fault Zone**

The southern SAF zone (Fig. 1) has been the locus of relative motion between the Pacific and North American plates since its inception in the Coachella Valley between ca. 6 and 12 Ma (e.g., Atwater, 1970; Stock and Hodges, 1989; Ingersol and Rumelhart, 1999; Oskin and Stock, 2003a, b). It consists of a main strand that bounds the northeast side of the Coachella Valley and Salton Trough, and is terminated at its southeast end in the Brawley seismic zone releasing step-over (Fig. 1). To the northwest of the study area, the southern SAF zone splits into the Banning and Mission Creek faults where the fault zone approaches a major restraining step-over in San Geronio Pass (Fig. 1).

Transtensional deformation over the past 6-12 Ma in the Salton Trough and Coachella Valley has resulted in rapid subsidence and creation of a very deep sedimentary basin beneath the modern valley floor (Fuis et al., 1984, 2012; Langenheim et al., 2005; Elders and Sass, 1988). Severe extension appears to have ruptured the lithosphere and deflected the Moho to shallower depths beneath the Salton Trough, resulting in filling of the basin with young (post-6 Ma) sediments and metasedimentary rocks to depths of ~10-12 km (e.g. Fuis et al., 1984; Dorsey, 2010). Basin fill of the southern Coachella Valley is highly asymmetric and tapers to the southwest where it onlaps basement rocks of the Santa Rosa Mountains (Langenheim et al., 2005).

The modern configuration of the southern San Andreas fault zone is the result of a complex Late Cenozoic history beginning with its inception in the Salton Trough at about

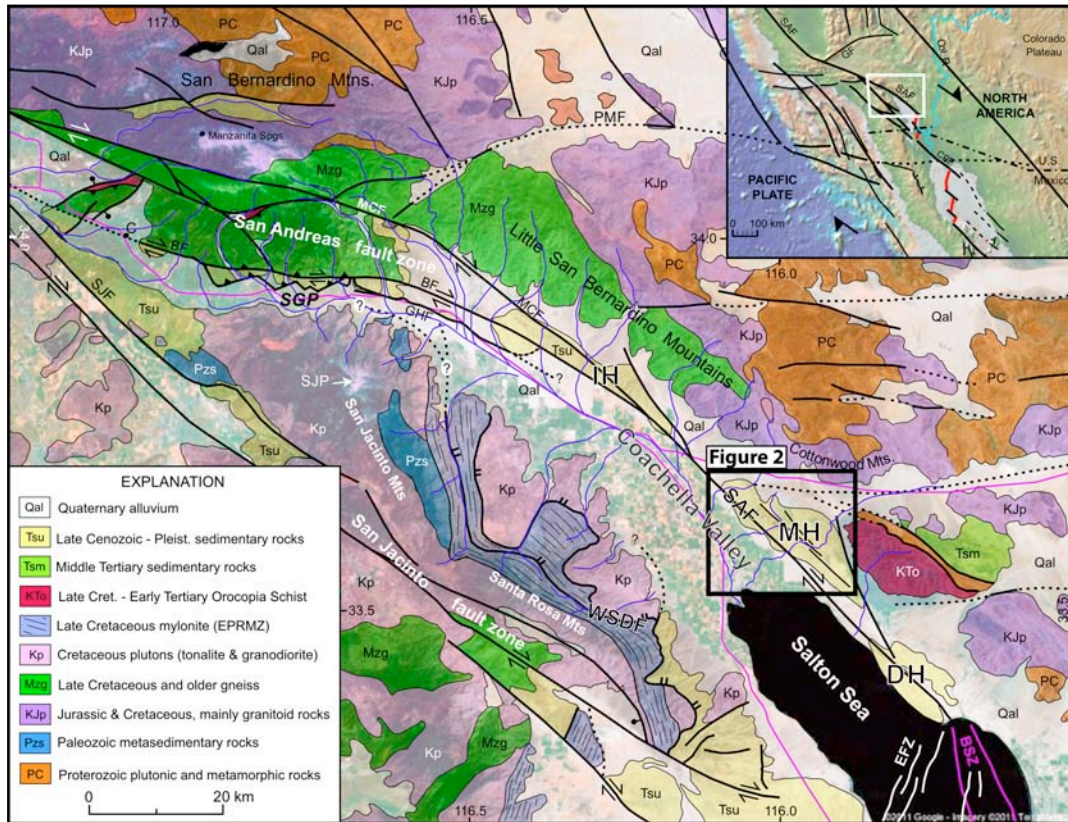


**Figure 1.** Geologic map of the Coachella. Modified from map compiled by Dorsey, 2011 (unpub.). Abbreviations: BF, Banning fault; BSZ, Brawley seismic zone; DH, Durmid Hill; EFZ, Extra fault zone; IH, Indio Hills; MCF, Mission Creek fault; MH, Mecca Hills; PMF, Pinto Mtn. fault; SAF, San Andreas fault; SGP, San Gorgonio Pass; SJF, San Jacinto fault; SJP, San Jacinto Peak; WSDF, West Salton detachment fault.

8 Ma (Axen and Fletcher, 1998; Dorsey et al., 2011). Regional transtension was partitioned into extension on the low-angle West Salton detachment fault and strike-slip offset on the SAF from latest Miocene to early Pleistocene time. At ~ 1.1 to 1.3 Ma a major reorganization of the southern San Andreas fault system resulted in initiation of the San Jacinto fault zone and termination of the West Salton detachment fault (e.g. Morton and Matti, 1993; Lutz et al., 2006; Janecke et al., 2010; Dorsey et al. 2011). It is speculated that a significant but uncertain fraction of the relative plate motion was transferred from the southern SAF to the San Jacinto fault zone at this time (Fig. 1).

Discrete elongate zones of fault-bounded uplifts along the southern SAF in the Indio Hills, Mecca Hills, and Durmid Hill define the northeast boundary of Coachella Valley and Salton Trough (Fig. 1). Between these uplifts, the geomorphic expression of the SAF varies from expressionless in lowland areas, to vegetation lineaments, dextrally offset geomorphic features, fault sags, and scarps (e.g. Sylvester and Smith, 1976; Keller et al., 1982; Sieh and Williams, 1990; Dibblee, 1997; Behr et al. 2010). Recent seismic imaging of the southern SAF (Fuis et al., 2012) and preliminary finite element modeling of fault kinematics through time (Fattaruso and Cooke, 2013) suggest that the Coachella valley strand of the SAF, previously assumed to be sub-vertical, may dip about  $65^\circ$  to the northeast. The implications of a northeast-dipping SAF in Coachella Valley remain unclear, but preliminary modeling suggests it may help explain recent uplift in the Indio, Mecca, and Durmid hill regions (Fattaruso and Cooke, 2013).

### **Mecca Hills**

The Mecca Hills are located on the northeast side of the Coachella Valley strand of the SAF, about 10 km north of the Salton Sea (Fig. 1). The topography of the Mecca Hills defines an elongate zone of heterogeneous strike-slip related deformation and uplift of Late Cenozoic terrestrial sedimentary rocks cut by high-angle sub-parallel faults and broad to tight en-echelon folds (Fig. 2; Sylvester and Smith 1976; Sheridan et al., 1994; Dibblee, 1997; Sylvester, 1999). Previous workers have proposed different models for transpressive deformation in the Mecca Hills. Sylvester and Smith (1976) concluded that upward-diverging and flattening oblique reverse faults, or ‘flower’ structures, are the dominant structural style in the Mecca Hills, with passive deformation of the sedimentary cover occurring above highly strained basement rock. Sheridan et al. (1994) noted the

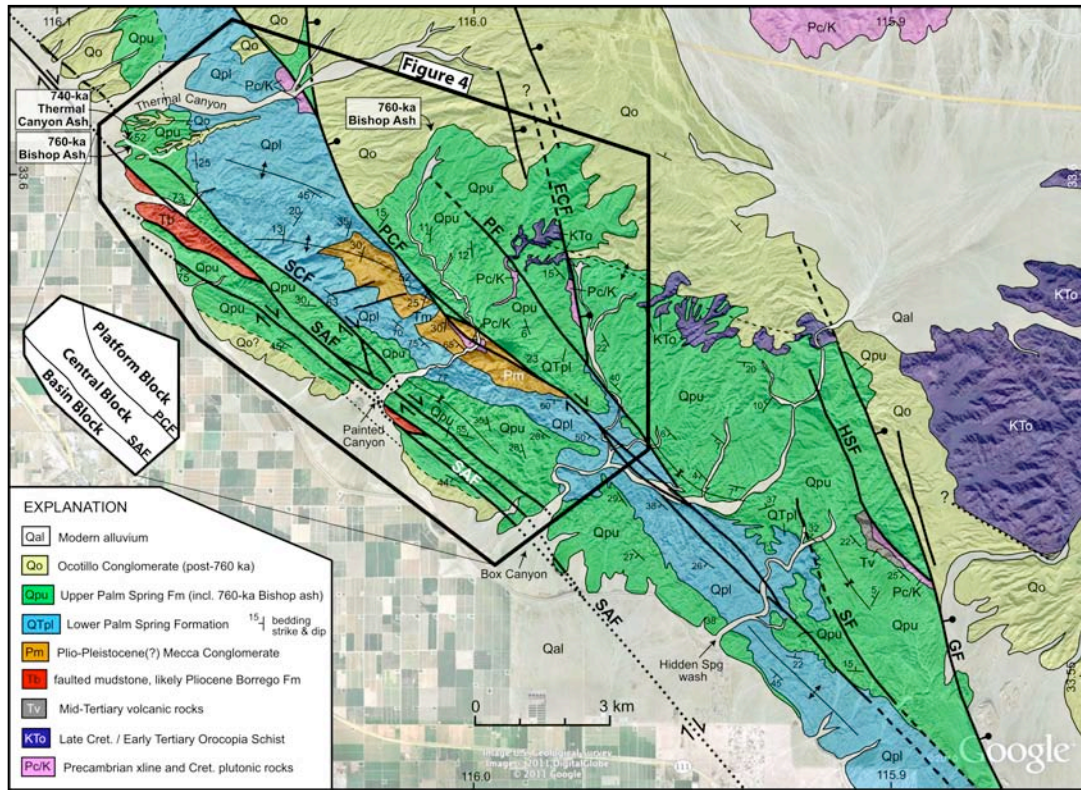


**Figure 2.** Geologic map of the Mecca Hills. Modified from map compiled by Dorsey, (2011, unpubl.). Inset map shows structural blocks from Sylvester and Smith (1927). Abbreviations: SAF, San Andreas Fault; SCF, Skeleton Canyon Fault; PCF, Painted Canyon Fault; PF, Platform Fault; ECF, Eagle Canyon Fault; HSF, Hidden Spring Fault; GF, Grotto Fault.

importance of inward-verging reverse faults and folds, or ‘pooch’ structures, formed by propagation of faults on the limbs of growing anticlines and rooted in weak sedimentary units. The major structures in the Mecca Hills are accompanied by smaller-scale transtensional horsetail splay faults, a feature typical of wrench-style tectonics (Fig. 2; Wilcox et al., 1973; Sylvester & Smith 1976; Sheridan et al., 1994; Miller, 1998).

A >1300-m thick continuous succession of sedimentary rocks is exposed in the Mecca Hills (Figs. 3, 4). This sequence includes the Mecca Conglomerate, Palm Spring Formation, and Ocotillo Conglomerate (Figs. 2, 3) first described by Dibblee (1954).





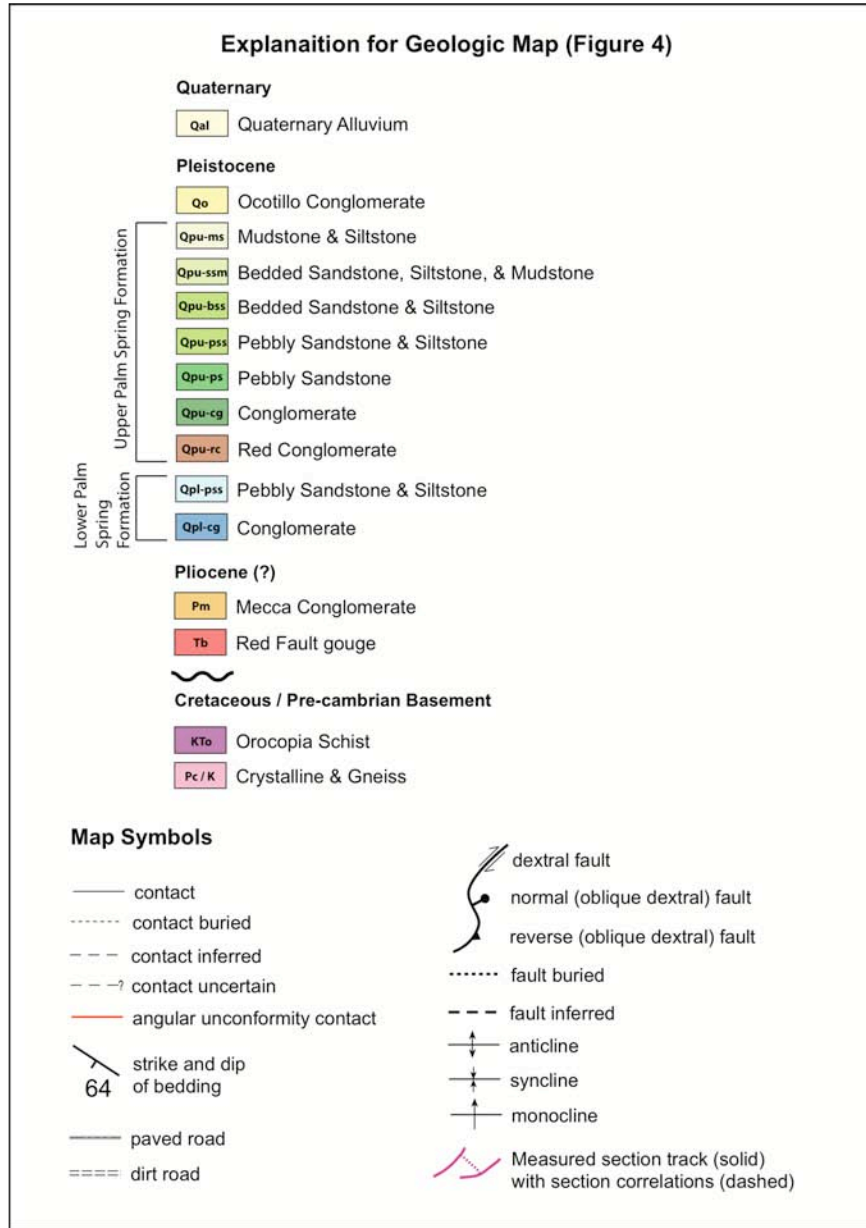


**Figure 4 (Continued).**

The main exposures of Mecca Conglomerate in the central Mecca Hills are limited to the southwest side of the Painted Canyon Fault (PCF), where it rests nonconformably on crystalline basement rock and grades up-section into the Palm Spring Formation in lower Painted Canyon (Figs. 3, 4). Previous workers suggested that coarse deposits exposed along Grotto and Hidden Spring faults in the southeast Mecca Hills are also equivalent to

the Mecca Formation (Boley et al., 1994). The lower member of the Palm Spring Formation conformably overlies the Mecca Formation and consists dominantly of interbedded sandstone and siltstone. A prominent angular unconformity separates the Palm Spring Formation into lower and upper members, and records an important phase of intra-basinal deformation within the fault zone (Figs. 3, 4). The Painted Canyon fault (PCF) is an important fault that appears to control the distribution of deposits and exposures of basement rock in the central to northwestern Mecca Hills (Figs. 4, 5).

Sylvester and Smith (1976) divided the central Mecca Hills into three structural blocks bounded by the SAF and PCF: (1) the Basin Block southwest of the SAF; (2) Central Block between the SAF and PCF, and (3) the Platform Block northeast of the PCF (Fig. 2). Each block contains a distinct stratigraphy and style of deformation. The Basin Block is deformed in a narrow belt of uplifted and eroding deposits along the southwest side of the SAF, and is otherwise mostly subsiding and buried beneath modern alluvium of the Coachella Valley. The Central Block contains the thickest exposed section of sedimentary rocks in the Mecca Hills, and is an area of intense transpressional deformation. The Platform Block consists of shallow basement with an overlying mostly undeformed cover of shallowly dipping ( $<15^\circ$ ) sedimentary rocks (Fig. 2).

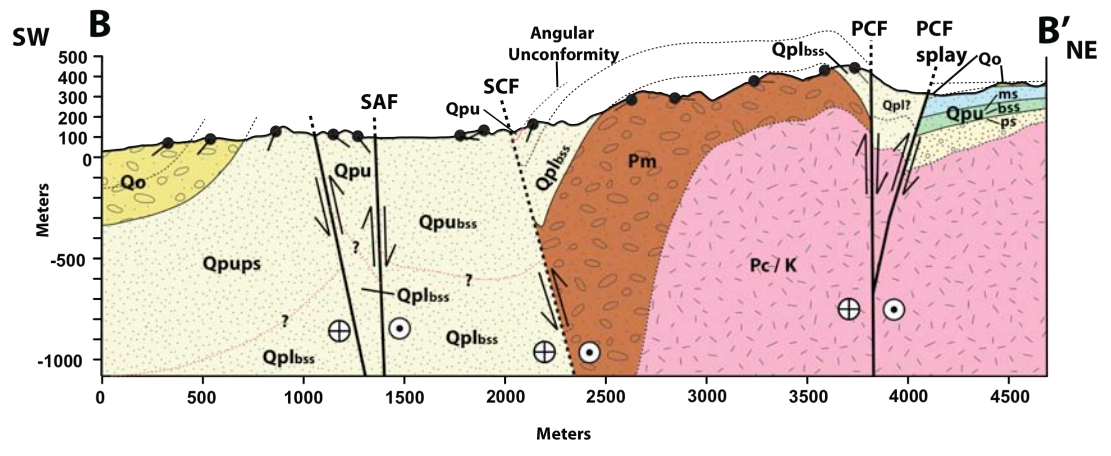
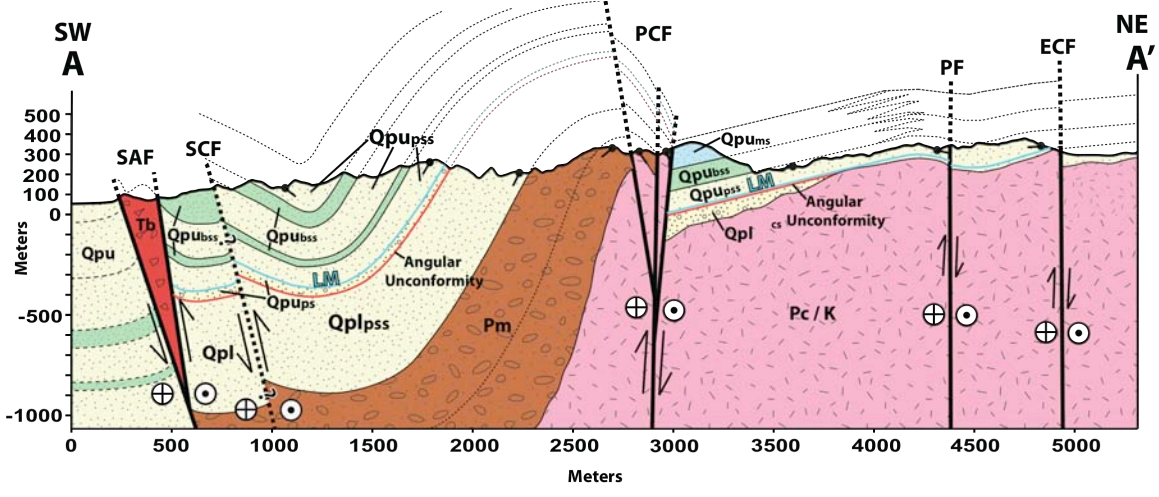


**Figure 5.** Geologic cross section from lines A-A' and B-B' in Figure 4. Abbreviations: SAF, San Andreas fault; SCF, Skeleton Canyon Fault; PCF, Painted Canyon fault; PF, Platform fault; ECF, Eagle Canyon fault.

## CHAPTER III

### METHODS

#### **Geologic Mapping**

Detailed geologic mapping of the central Mecca Hills was conducted in the field over the course of two field seasons in 2012 and 2013. Figure 4 is a geologic map of the central to northwestern Mecca Hills produced during this study. Stratigraphic formations, sub-facies, and geologic contacts were mapped on high resolution Google Earth satellite imagery with UTM grid overlay at 1:10,000 scale. Bedrock exposures permit some contacts to be inferred from satellite imagery, which was useful when mapping inaccessible high-relief areas.

#### **Measured Stratigraphic Sections**

Stratigraphic sections were measured in the field with a 1.5-m Jacob's staff at the meter to sub-meter scale, accompanied by detailed facies descriptions. Section 1 is a composite of 5 sections measured northeast of the PCF (Fig. 4) that were correlated using distinct marker horizons. Due to low bedding dips, Section 1 spans a large area and crosses significant lateral facies changes. In order to constrain facies architecture in this area, several short intervals within section 1 were measured with photography in vertical cliff exposures where direct measurements were unattainable. This technique allowed us to correlate lateral facies changes from southeast to northwest that are visible high in the canyon walls but not exposed at ground level. Section 3 was measured in lower Painted Canyon perpendicular to the strike of bedding (Fig. 4).

## **Paleocurrents & Clast Counts**

Determination of paleocurrent directions was conducted by measuring (1) the strike and dip of imbricated clasts in conglomeratic beds, (2) strike and dip of cross-bed foresets, (3) trend and plunge of current lineations and tool marks on the base of beds, and (4) trend and plunge of fluvial channel axes. Imbricated clast and cross-bed foreset measurements provide unique paleoflow directions, while current lineations, tool marks, and fluvial channel axes must be coupled with other data to determine a unique paleoflow direction.

Conglomerate clast counts were conducted by establishing a ~ 1 m square on rock outcrops, randomly selecting at least 100 clasts using a systematic grid system, and tallying relative abundances of various compositions. The most distinctive composition is Orocopia Schist sourced from local basement and the Orocopia Mountains southeast of the Mecca Hills. Other compositions of pre-Cambrian to Cretaceous plutonics and Tertiary volcanic rocks are sourced from local basement and the Cottonwood Mountains (fig. 1).

## **Paleomagnetic Analysis**

Previous attempts to date deposits in the Mecca Hills have been partially successful, and were based on the presence of the 760-ka Bishop Ash high in the section and the abundance of reversed magnetic polarity sites thought to represent the Matuyama subchron (2.58- to 0.78-Ma; Chang et al., 1987; Boley et al., 1994). These constraints were used to conclude that much of the upper member of the Palm Spring Formation exposed in the Mecca Hills was deposited between 0.76- and 2.58 Ma (Chang et al., 1987; Boley et al., 1994). Boley (1993) and Boley et al. (1994) documented strong

normal-polarity overprinting in many of their paleomagnetic samples of the Palm Spring Formation in the Mecca and Indio Hills, suggesting that magnetic overprinting may affect much of the Palm Spring Formation. They found step-wise thermal demagnetization to be much more effective at removing magnetic overprints in their samples than alternating-field demagnetization.

Realizing the issues raised by prior paleomagnetic studies in the Mecca Hills, we tentatively use recently acquired magnetostratigraphic data (Messe et al., 2012) for sections 1 and 3. Samples were collected in the field using three methods: (1) using a handheld gasoline powered drill to sample 1-inch diameter oriented cores; (2) collection of oriented block samples that were later drilled in the lab; and (3) use of 1-inch diameter by 1-inch deep plastic collection cylinders to collect poorly indurated sediments.

Sampling of Section 3 yielded 57 drilled core sites and 1 oriented hand sample site, with an average stratigraphic spacing of ~22 m between sampled sites. Due to the restricted access for the gasoline-powered drill in Section 1, these samples consist of 40 oriented hand sample sites and 7 plastic cylinder sample sites with an average stratigraphic spacing of ~15 m between sites. The number of samples varied between sites based on sampling technique and rock quality. On average we collected 4-6 cores at drill sites, 1-5 blocks and oriented block sites, and 5-7 plastic tubes at soft-sediment sites.

Samples were analyzed by Bernie Housen and Graham Messe at Western Washington University, using alternating-field and thermal demagnetization techniques to determine the original magnetic polarity of the deposits. The plastic tube samples cannot be thermally demagnetized, and since alternating-field demagnetization appears to be ineffective at removing magnetic overprints, we remove these sites (Fig. 6A) from our

analysis until further analysis can show convincing original polarities. The remaining paleomagnetic data, coupled with the presence of the Bishop Ash high in Section 1, are used to estimate sediment-accumulation rates and ages for sedimentary rocks in the central Mecca Hills. We use these preliminary magnetostratigraphic data at face value. The results will likely be refined and modified pending further sample analyses and confidence tests.

## CHAPTER IV

### RESULTS

#### **Geologic Map and Cross Sections**

The geologic map (Fig. 4) and cross sections (Fig. 5) provide important context for analysis and interpretation of sedimentary rocks in this study. Sedimentary rocks in the central Mecca Hills nonconformably overlie Pre-Cambrian and Cretaceous basement rocks in a >1300-m thick succession that records late Cenozoic terrestrial sedimentation over the past 4 - 5 Ma. Previous workers noted the diversity of facies and abrupt lateral and vertical facies changes in the Mecca Hills, especially in relation to structures (Sylvester & Smith, 1976; Chang et al., 1987; Sheridan et al., 1994; Boley et al., 1994). Our mapping confirms the contrast between the diverse localized facies distributions of the upper member of the Palm Spring Formation, and the widespread relatively uniform facies distribution of the lower member of the Palm Spring Formation in the central Mecca Hills (Fig. 4), similar to the findings of previous workers in the southeast Mecca Hills (e.g. Chang et al., 1987; Sheridan et al., 1994; Boley et al., 1994). Our geologic cross sections (Fig. 5) help to refine the distribution of sedimentary sequences, basement relationships, and structural styles of the Platform, Central, and Basin blocks. Measured stratigraphic sections produced during this study are presented in Figure 6A, B. In the following section we describe and interpret the Mecca Conglomerate, Palm Spring Formation, and Ocotillo Conglomerate based primarily on observations of exposures in the central Mecca Hills near Painted Canyon (Fig. 2, 4).

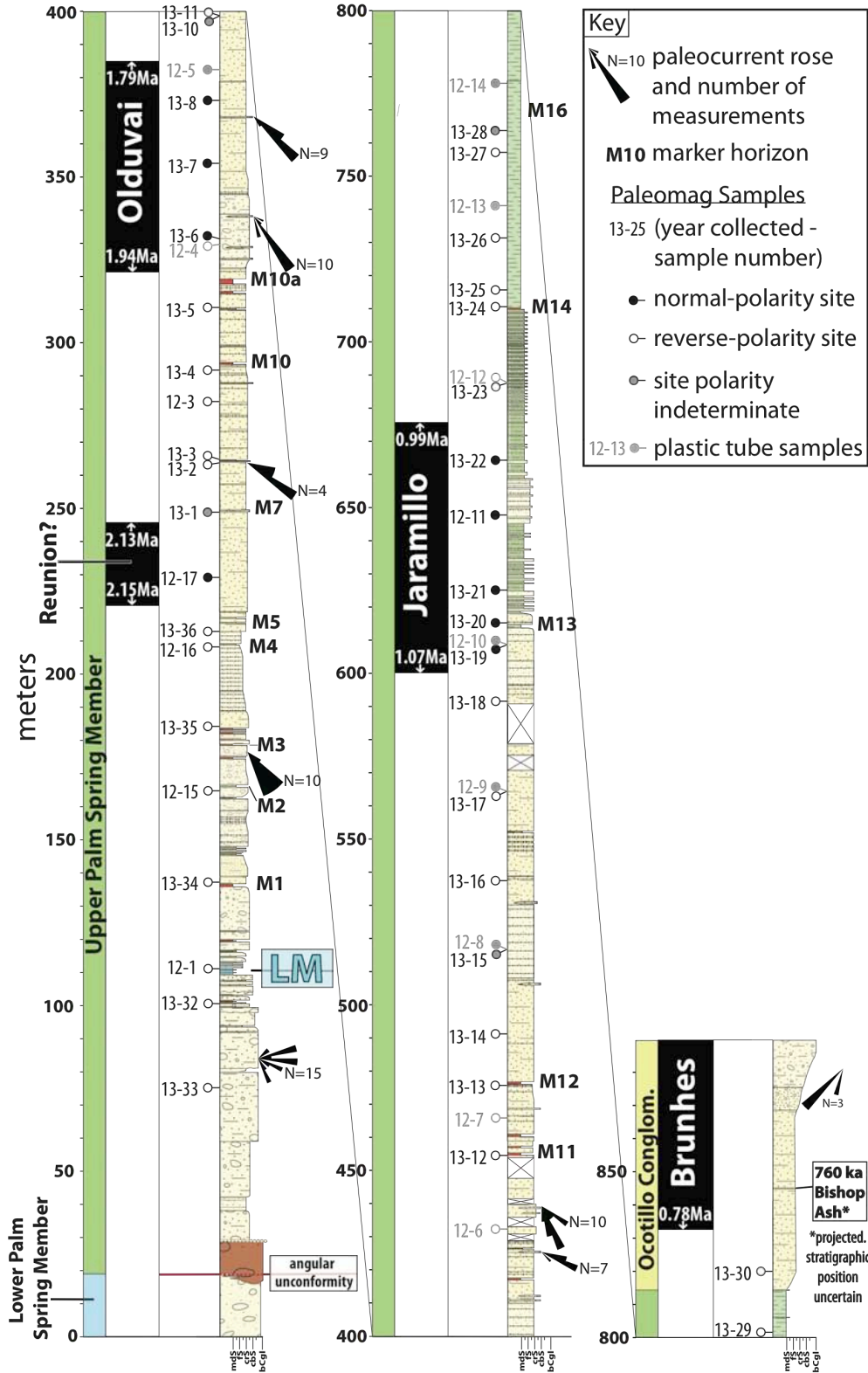


**Figure 6.** (A) Measured stratigraphic Section 1, northeast of the Painted Canyon Fault with our preferred correlations to the Geomagnetic Polarity Time Scale (GPTS), and estimated ages for limestone LM and the angular unconformity.

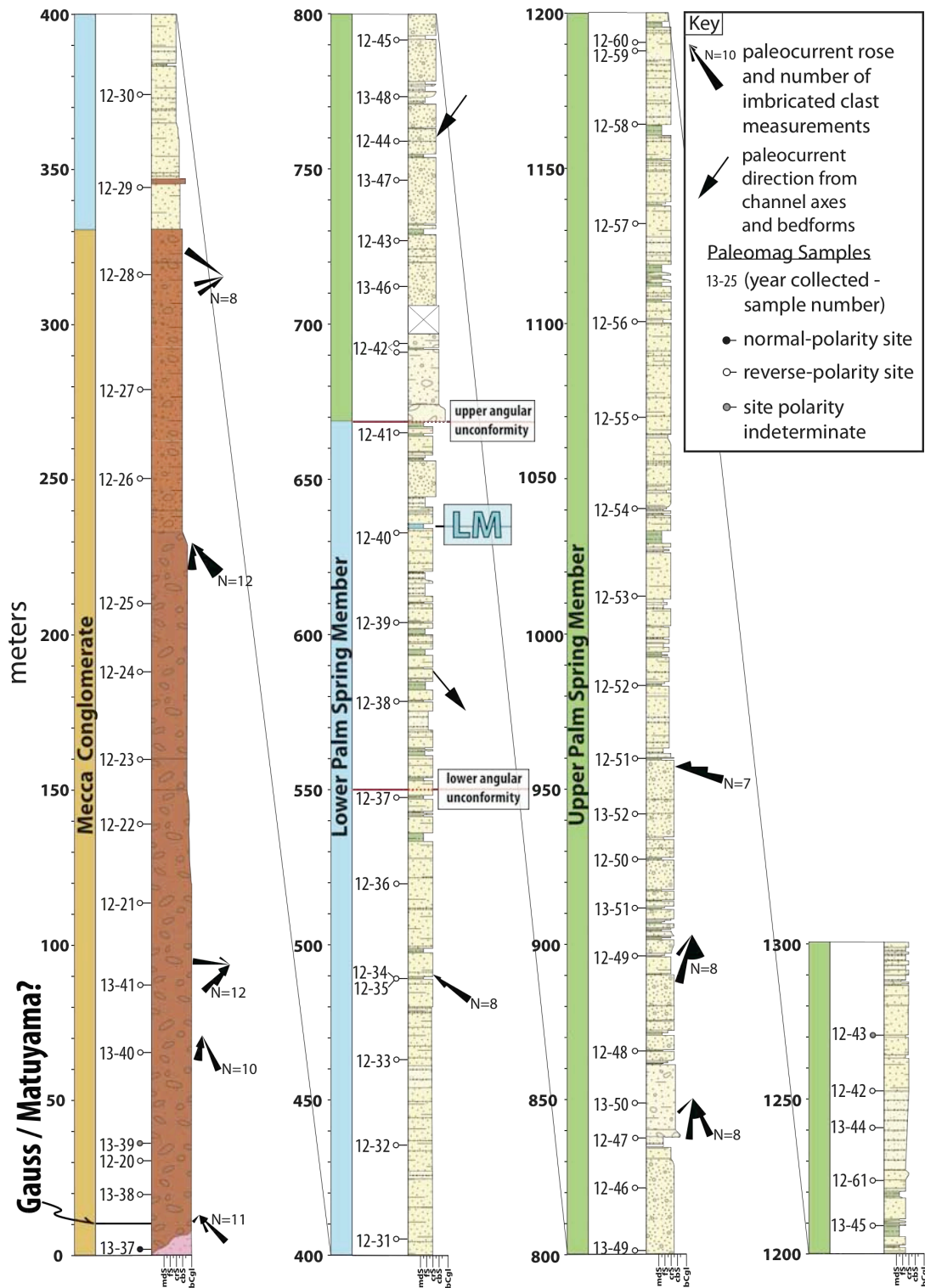


**Figure 6 (Continued). (B)** Measured stratigraphic Section 3 with our preferred calculated ages for the base of the Mecca Conglomerate, base of the lower Palm Spring member, lower angular unconformity, limestone LM, upper angular unconformity (base of upper Palm Spring member).

## **Sedimentary Lithofacies**

### ***Mecca Conglomerate (Pm)***

The oldest record of sedimentation exposed in the central Mecca Hills is the Mecca Conglomerate, which rests nonconformably on basement rock in lower Painted Canyon (Fig. 4) with a total measured thickness of 330 m (Fig. 6). The lower ~150 m consists of poorly sorted, weakly bedded (~5 - 10 m thick), interbedded pebble-cobble to small-boulder conglomerate and pebbly sandstone with dominantly gneissic clasts with lesser granitic and Orocopia Schist clasts derived from nearby basement (Table 1A, Fig. 6B, Fig. 7A). The upper ~180 m consists of dominantly pebble to cobble conglomerate with better-defined bedding ranging from ~1 to 5 m thick. Imbricated clasts indicate a dominant paleoflow to the south-southwest with lesser west and northwest paleoflow directions (Fig. 6B). The Mecca Conglomerate in lower Painted Canyon is interbedded with and gradationally fines up-section into the overlying lower member of the Palm Spring Formation (Fig. 6B).

We conclude that the lower part of the Mecca Conglomerate was deposited by debris flow dominated proximal alluvial fans, based on the abundance of poorly sorted, weakly bedded conglomerate (e.g., Blair, 1987a), and the approximately radial pattern of paleocurrent directions (fig. 6A) that suggest deposition emanating from a point source. Locally-derived clast compositions and overall southwest-directed paleocurrent directions suggest that coarse gravelly deposits were derived from the northeast, likely from the northeast side of the PCF. The overall fining-up trend records a gradual transition from a proximal to distal alluvial-fan environment and depositional processes.

**Table 1. (A)** Descriptions and interpretations of sedimentary rock facies in the study area

Lithic Designator	Description	Interpretation
<b>Qpu-ps</b>	<b>Upper Palm Spring Pebbly Sandstone:</b> Horizontally stratified very coarse-grained pebbly sandstone in broad flat-based, convex-up, amalgamated sheets (5- to 40-cm thick) with pebble stringers and rounded clast-supported rounded cobble-conglomerate channel fills (<1-m thick).	Medial alluvial fan
<b>Qpu-cg</b>	<b>Upper Palm Spring Conglomerate:</b> Horizontally stratified, amalgamated, sub-angular, dominantly matrix-supported, cobble to boulder conglomerate. Felsic-plutonic and gneissic clasts in the NE Mecca Hills (typically < 0.5 m).	Proximal to medial alluvial fan
<b>Qpu-rc</b>	<b>Upper Palm Spring Red Conglomerate:</b> Horizontally stratified to massive, sub-angular, dominantly matrix-supported cobble to boulder conglomerate composed of entirely Orocopia Schist debris.	Proximal alluvial fan
<b>Qpl-pss</b>	<b>Lower Palm Spring Pebbly Sandstone &amp; Siltstone:</b> Very coarse-grained to pebbly and occasional cobble trough cross-bedded sandstone (1- to 6-m thick) and with interbedded 0.5- to 4-m thick laminated and ripple-cross laminated, biotite-rich green medium sandstone and siltstone. Bedding is uniform and tabular, and individual beds are traceable for several km's.	Fluvial and overbank fines
<b>Qpl-cg</b>	<b>Lower Palm Spring Conglomerate:</b> Horizontally stratified to massive, sub-angular, dominantly matrix-supported cobble to boulder conglomerate composed of dominantly felsic-plutonic and gneiss clasts.	Proximal alluvial fan
<b>Pm</b>	<b>Mecca Conglomerate:</b> Maroon colored, poorly sorted, sub-angular to sub-rounded, cobble to small boulder conglomerate. Low in section dominated by clast supported (clasts < 0.5 m), poorly developed planar bedding (< 3-m thick) with sharp non-erosive bases and lacking internal sedimentary structures (except imbricated clasts). Grades into dominantly matrix supported (clasts < 20 cm) conglomerate, better developed bedding (< 1.5 m thick) with increased small very coarse-grained sandstone channel fills.	Proximal alluvial fan

**Table 1 (Continued). (B)**

Lithic Designator	Description	Interpretation
<b>Qo</b>	<p><b>Ocotillo Pebbly Sandstone and Conglomerate:</b> Very coarse horizontally stratified pebbly sandstone at base ( 0- to 65-m thick ), coarsening to very poorly sorted, sub-rounded, matrix-supported, very poorly indurated boulder conglomerate with clasts up to 1 m ( 20- to 30-m thick ). Felsic-plutonic and gneissic clasts in the NE Mecca Hills, and Orocopia Schist clasts in the SW Mecca Hills.</p>	Proximal to medial alluvial fan
<b>Qpu-ms</b>	<p><b>Upper Palm Spring Mudstone and Siltstone:</b> Laminated claystone, mudstone, and siltstone. Occasional burrows, mottling, and gastropod fossils. Lacks desiccation features.</p>	Shallow lacustrine
<b>Qpu-mss</b>	<p><b>Upper Palm Spring Mudstone, Siltstone, &amp; Sandstone:</b> Horizontally stratified mudstone, laminated siltstone, and featureless to moderately normal-graded medium- to fine-grained sandstone. Lacks desiccation features.</p>	Shallow lacustrine with coarser input from flash-flood events
<b>Qpu-bss</b>	<p><b>Upper Palm Spring Bedded Sandstone and Siltstone:</b> Moderately normal-graded medium- to coarse-grained sandstone (0.2- to 1-m thick) fining to ripple cross-laminated biotite-rich green siltstone 5- to 10-cm thick. Also, Horizontally stratified featureless 5- to 20-cm thick medium-grained sandstone with interbedded 5- to 20-cm thick laminated to mottled and desiccated siltstone. Burrows and root casts common.</p>	Very distal alluvial fan sheetflood deposits for normally graded sandstone facies, and nearshore to very shallow lacustrine for thinner featureless sandstone facies
<b>Qpu-pss</b>	<p><b>Upper Palm Spring Pebbly Sandstone &amp; Siltstone:</b> Horizontally stratified amalgamated sheets of very coarse-grained to mildly pebbly sandstone of variable thickness with interbedded 1- cm to 1.5-m thick green laminated to ripple-cross laminated siltstone. Occasional small (~1.5-m wide, ~20-cm deep) clast-supported pebble to cobble conglomeratic channel fills. Calcic paleosols common.</p>	Distal alluvial fan

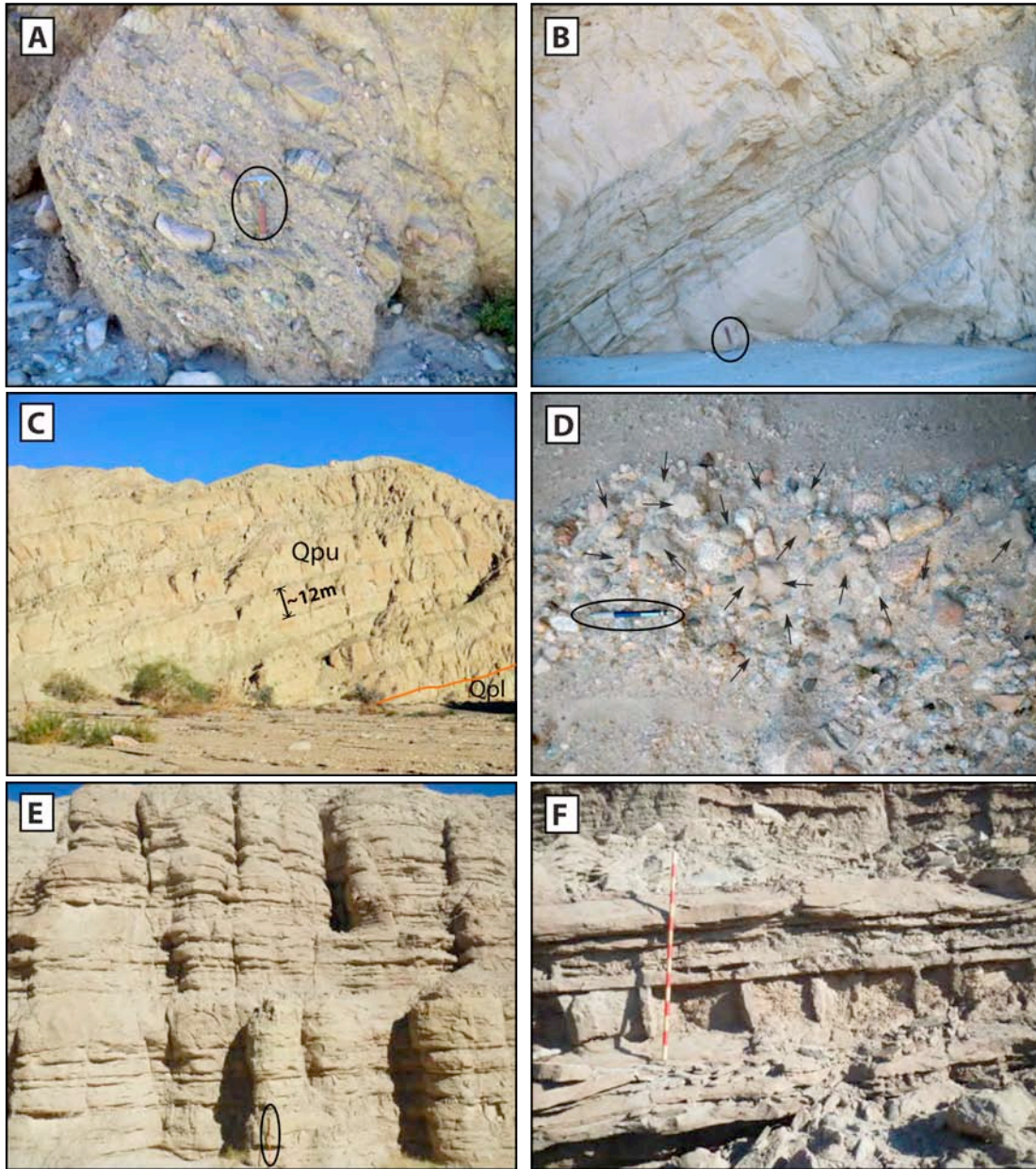


**Figure 7.** Photographs of sedimentary rocks exposed in the Mecca Hills. A) Mecca Conglomerate in lower Painted Canyon. Hammer circled for scale. (B) Fining upward sequence from pebbly sandstone to siltstone in the lower member of the Palm Spring Formation. Hammer circled for scale. (C) Interbedded pebble – cobble sandstone and siltstone of the upper member of the Palm Spring Formation (Qpu) exposed in Box Canyon. Red line indicates angular unconformity separating the upper and lower (Qpl) members. (D) Abundant sandstone clasts of the lower member in conglomerate of the upper member northeast of the PCF. Pencil circled for scale (E) Medium-bedded sandstone and siltstone of the upper member northeast of the PCF (1.5-m Jacob’s staff circled). (F) Thinly-bedded sandstone with desiccated siltstone and mudstone of the upper member northeast of the PCF.

### ***Palm Spring Formation***

The most widely exposed sedimentary unit in the Mecca Hills is the Palm Spring Formation, which consists of a lower and upper member that are separated by a persistent angular unconformity (Figs. 4, 6B, 8E). The unconformity marks the boundary between regionally extensive and relatively uniform facies of the lower member and highly variable, localized facies of the upper member observed in the central Mecca Hills.

#### ***Lower Member, Palm Spring Formation (Qpl)***

The lower member of the Palm Spring Formation is 340 m thick in lower Painted Canyon where it conformably and gradationally overlies the Mecca Formation on the southwest limb of Mecca Anticline (Figs.4, 6B). The lower member consists of tabular, uniformly bedded couplets consisting of grus-like, cross-bedded pebbly sandstone with plutonic and gneissic clasts that fines up into biotite-rich green sandstone and siltstone (Table 1A, Fig. 7B). Individual beds are laterally continuous with sharp boundaries that are traceable for several km's along strike, typically with little change in facies. Paleocurrent indicators suggest southeast-directed transport (Fig. 6B). The lithofacies assemblage and stratal architecture of the lower member in the central Mecca Hills is similar to that seen in the Indio Hills 25 km to the northwest, providing evidence for its regional extent. Exceptions to this are observed in Eagle Canyon where the lower member consists of poorly sorted cobble to boulder conglomerate (Table 1A), and in the southeast of the study area near Hidden Spring Wash (Fig. 2) where similar coarse facies have been previously documented (Chang et al., 1987; Sheridan et al., 1994).

The laterally extensive tabular sheets of cross-bedded sandstone and siltstone in the lower member suggest deposition in a fluvial system comprised of a migrating

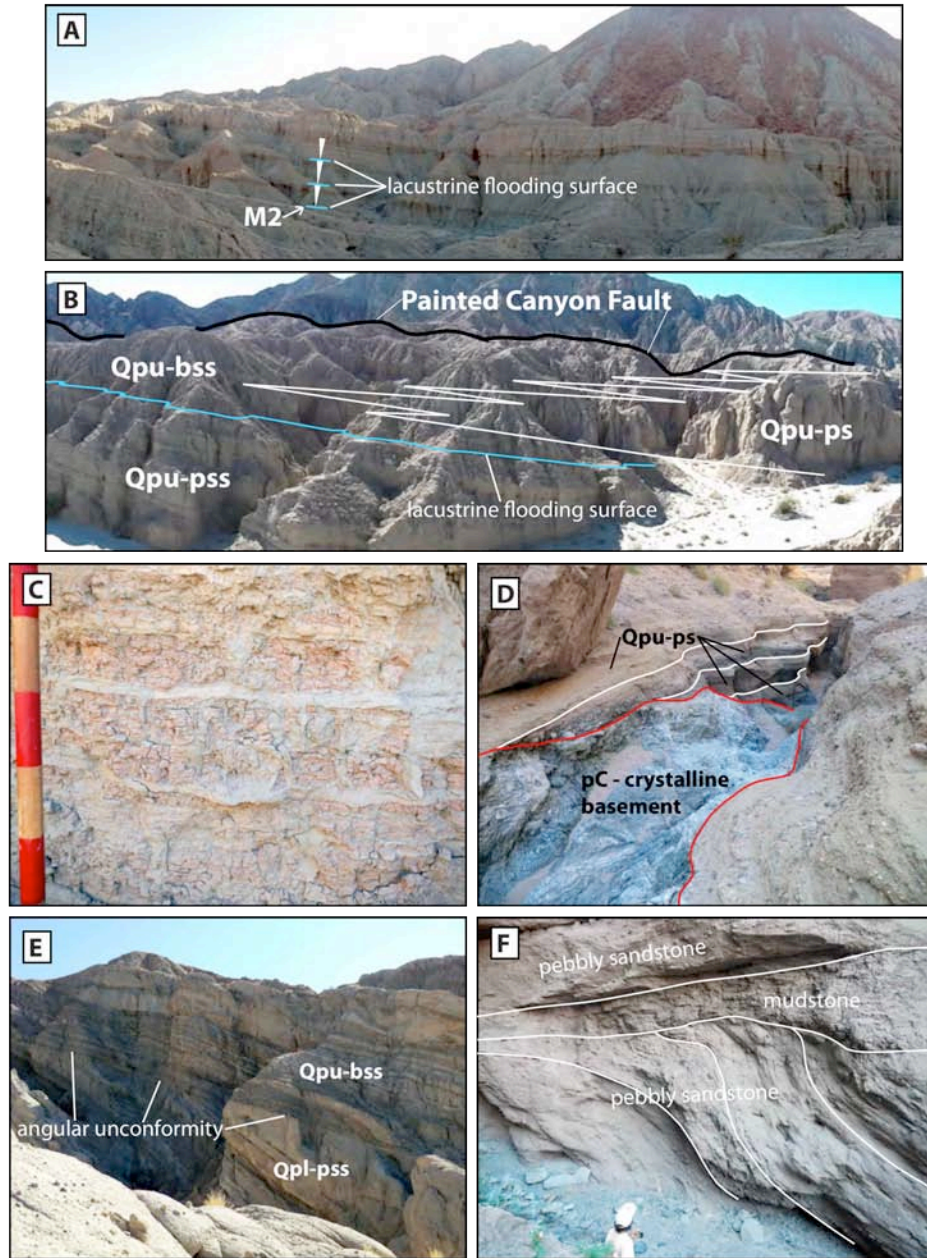


**Figure 8.** Photographs of stratigraphic relationships in the Mecca Hills. (A) Coarsening upward sequences in lacustrine and nearshore deposits capped by lacustrine flooding surfaces between Eagle Canyon and the PCF. (B) Medial alluvial fan deposits (Qpu-pss) capped by lacustrine flooding surface and lateral interfingering of nearshore bedded sandstone and siltstone (Qpu-bss) with distal alluvial fan deposits (Qpu-ps) of the upper member of the Palm Spring Formation. (C) Sandstone-filled mudcracks in dessicated mudstone of marker horizon M10a. 10-cm-long divisions on Jacob's Staff for scale. (D) Upper member of the Palm Spring Formation onlapping basement northeast of the PCF. (E) Angular unconformity separating lower from upper Palm Spring Formation near Box Canyon. (F) Angular truncation of sandstone beds capped by mudstone if the upper member of the Palm Spring Formation northeast of the PCF.

channel (cross-bedded sandstone) and adjacent overbank floodplain (green siltstone) that occupied a broad basin floor. These geometries permitted widespread lateral migration of channels and created a very broad sheet-like fluvial architecture (e.g., Miall, 1985; Hampton & Horton, 2007). The combination of felsic-plutonic and gneissic clasts with southeast-directed paleocurrent directions suggests that the finer, uniform facies of the lower member of the Palm Spring Formation were deposited in a large river system that flowed southeast down the paleo-Coachella Valley into the Salton Trough, with sources mainly in the Cottonwood and Little San Bernardino Mountains. The local coarse facies of the lower member likely were deposited in proximal basin-margin alluvial fans.

***Upper Member, Palm Spring Formation (Qpu)***

The upper member of the Palm Spring Formation contains a wide range of lithofacies types displaying abundant vertical and lateral variability, in contrast to the regionally uniform nature of the lower member. The contrast between deposits on the southwest and northeast sides of the PCF makes reliable correlations of upper Palm Spring across the PCF difficult. One exception to this is a distinct limestone bed (LM) observed northeast of the PCF near Eagle Canyon (110 m Section 1, Figs. 4, 6A), and southwest of the PCF in Painted canyon (635 m Section 3, Figs. 4, 6B). The ~3-m thick limestone bed is characterized by horizontally stratified ~1- to 5-cm thick beds of platy white limestone interbedded with thin (<5-mm) green siltstone in the lower ~1.5 m that coarsen to >10-cm thick medium sandstone interbeds in the upper ~1.5 m. Limestone beds consist of ~3-mm thick flakey calcite lamina (possibly varves) with rare burrows, and is comprised almost entirely of calcareous bladed fossil plant material that appear to be grasses. Correlation of the limestone across the PCF is based on its unique and

laterally persistent lithologic characteristics, the obvious similarities between exposures on both sides of PCF, and its stratigraphic position ~80 – 90 m above an angular unconformity observed on both sides of the PCF (Fig. 6A, B).

Southwest of the PCF in lower Painted Canyon, the upper member of the Palm Spring Formation is > 700 m thick and fines up-section from coarse conglomeratic sandstone with channel-fill conglomerate to very coarse-grained planar and cross-bedded pebbly sandstone and interbedded green ripple-cross laminated siltstone (Fig. 7C), with abundance of siltstone interbeds increasing up-section (Table 1A, B, Fig. 6B). Thin coarsening-up intervals (0.5 -1.5 m) of claystone to medium-grained sandstone become increasingly abundant beginning at 860 m in Section 3 (Fig. 6B). Imbricated clasts, channel scours, cross-bedding foresets, tool marks, and flute casts all indicate paleoflow to the south-southwest to south-southeast (Fig. 6B).

The coarsest facies of the upper Palm Spring member southwest of the PCF suggest deposition in a proximal to distal alluvial fan system (e.g., Blair, 1987a). Higher in the section (Fig. 6), horizontally stratified and cross-bedded coarse-grained sandstone and siltstone may represent distal alluvial fan to fluvial environments (e.g., Nichols & Hirst, 1998) near the margin of a paleo-lake in the Salton Trough. The thin coarsening upward intervals of claystone and medium-grained sandstone are inferred to record short-lived lake highstands followed by rapid southeast progradation of distal alluvial fans into the lake.

Northeast of the PCF, the base of the upper Palm Spring member near Eagle Canyon consists of locally preserved, channelized red cobble-boulder conglomerate that abruptly fines up-section into very coarse-grained, medium-grained, and very fine-

grained facies (Table 1A, Fig. 4, Fig. 6A). This conspicuous basal red boulder conglomerate is exposed on the southwest side of Eagle Canyon at the contact between the lower and upper members, and resembles similar conglomerates above the unconformity in the southeast Mecca Hills (Chang et al., 1987; Sheridan et al., 1994). It has a scoured base, is typically less than ~ 30-m thick, and contains exclusively Orocopia Schist clasts with southwest-directed paleocurrent indicators (Fig.6). A cobble-lag cap separates it from more uniform and widely distributed overlying deposits of the upper member.

Very coarse-grained deposits of the upper member exposed in upper Painted Canyon consist of horizontally stratified pebble-cobble conglomerate that grade laterally into planar amalgamated, very coarse-grained pebbly sandstone (Table 1A, B, Fig. 4). Calcic paleosols and laterally extensive ~ 0.5- to 2-m thick heavily desiccated red mudstone beds are irregularly interbedded with the coarser facies of the upper member (Fig. 8C). Clast compositions are dominantly felsic-plutonic and gneiss. In addition, clasts of reworked sandstone first appear in conglomeratic channel fills several meters beneath marker horizon M10a (Fig. 7D, Fig. 6A), within 280-m map distance northeast of the PCF (Fig. 4). While other sandstone clasts likely sourced from the Miocene Diligencia basin to the east (Law et al., 1996) have been found in the Palm Spring Formation, we infer that these sandstone clasts were eroded from the lower member of the Palm Spring Formation because of their compositional and textural similarity to the lower member and their proximity to the PCF. Imbricated clasts in conglomerate of the upper member in upper Painted Canyon record consistent southeast paleoflow, roughly parallel to the trace of the PCF (Fig. 4, Fig. 6).

Medium-grained facies of the upper member comprise two distinct variants of bedded sandstone and siltstone. The first variant consists of well-bedded, normal-graded sandstone (0.2- to 1.5-m thick) with thin (1- to 5-cm thick) interbedded siltstone (Fig. 7E), and the other consists of bedded internally structureless sandstone (5- to 20-cm thick) with interbedded desiccated siltstone and mudstone (4- to 50-cm thick) (Table 1B, Fig. 7F). The finest-grained facies are preserved as 20- to 30-m thick coarsening-upward sequences of laminated claystone, mudstone, siltstone, and coarse-grained sandstone low in section 1 (Table 1B, Fig. 8A). In northwestern-most upper Painted Canyon, similar fine-grained facies comprise a ~200-m fining-upward sequence from laminated siltstone to mudstone to claystone (Fig. 6A).

We infer that the red basal conglomerate was deposited during a brief episode of southwest-directed transport in alluvial fans derived from local Orocopia Schist basement sources (Fig. 2), based on distinctive southwest paleocurrent directions and Orocopia Schist clast compositions. Coarse pebble conglomerate and pebbly sandstone of the upper member northeast of the PCF were deposited in the medial to distal reaches of alluvial fans, respectively (e.g. Blair & McPherson, 1994), that were transported southeast. Rapid lateral fining of horizontally stratified conglomerate to planar pebbly sandstone with reworked conglomeratic channels is consistent with down-transport facies associations observed in active alluvial fans (Blair, 1987a). Clast compositions and southeast-directed paleocurrent indicators suggest the fans were sourced from the Cottonwood Mountains (Fig. 1). The thicker normal-graded sandstone and siltstone variants (Fig. 7E) are interpreted as sheetflood deposits that accumulated in a distal alluvial fan and sand-flat setting (e.g., Blair & McPherson, 1994). The thinner featureless sandstone, siltstone, and

mudstone facies (Fig. 7F) are interpreted as near-shore mudflat deposits that accumulated at the most distal reaches of alluvial fans. In this setting, sheet sands were deposited by flash floods on a desiccated mudflat or in very shallow water by hyperconcentrated grain-flows (e.g., Mulder & Alexander, 2001). We infer that the finest-grained facies were deposited by suspension settling in a shallow lacustrine environment based on dominance of laminated fine-grained mud and silt and lack of desiccation features.

### ***Ocotillo Conglomerate (Qo)***

The Ocotillo Conglomerate ranges in thickness from ~5 to >65 m and consists of very coarse-grained, horizontally stratified sandstone that coarsens up section to poorly sorted pebble-cobble-boulder conglomerate (Table 1B). Clast compositions are entirely felsic-plutonic and gneissic with southwest-directed paleocurrent indicators in the northwest and northeast Mecca Hills (Fig. 6A). On the southwest side of the SAF northwest of Painted Canyon, Ocotillo Conglomerate consists of large, several-km-wide, overlapping units of horizontally stratified conglomeratic sandstone distinguished by one set dominated by felsic plutonic and gneissic clasts and the other set containing almost entirely Orocopia Schist clasts. In the southeast Mecca Hills there are many conglomerate facies that interfinger with the Palm Spring Formation and persist up to the present day alluvial fans, and while the latest progradation of these fans may be linked to Ocotillo Conglomerate progradation, they are a generally a much older lithostratigraphic unit.

The erosional base and widespread thin sheet-like geometry of the Ocotillo Conglomerate records basinward progradation of gravels sourced in nearby mountains. In the northeast Mecca Hills this unit represents the gravelly deposits of a southwest-transported alluvial fan system sourced in the Cottonwood Mountains, northeast of the

Mecca Hills (Fig. 2). Southwest of the San Andreas Fault the Ocotillo Conglomerate likely has been translated a significant distance northwest by right-lateral fault slip from its original depositional location. Here, the alternation of contrasting clast compositions and basin-ward paleocurrent indicators in the Ocotillo Conglomerate suggest it was deposited in overlapping alluvial fans sourced from the Cottonwood Mountains (felsic-plutonic clast source) and Orocochia Mountains (Schist clast source).

### **Stratigraphic and Basinal Architecture**

#### ***Lacustrine Sequence, Upper Member Palm Spring Formation***

Facies associations of the upper member northeast of the PCF in the central Mecca Hills define a retrogradational architecture that records transgression and retreat of a lake shoreline to the northwest, parallel to the PCF. This transgression is recorded in deposits from the southeast near Eagle Canyon to the upper end of Painted Canyon wash where it crosses the PCF (Fig. 4, Fig. 9). Fine-grained lacustrine and near-shore facies exposed low in Section 1 near Eagle Canyon (Fig. 8A) coarsen over a short distance to the northwest into laterally equivalent distal and medial alluvial fan facies (bedded sandstone and pebbly sandstone). This lateral transition migrates laterally up section from southeast to northwest, from Eagle Canyon (Fig. 8B) to the northwestern upper Painted Canyon where exposures are limited to high canyon walls or are missing due to erosion.

Farther up-section, medial to distal alluvial fan facies dominate most of the exposures in upper Painted Canyon, with thin interbedded units of nearshore lacustrine mudstone (Fig. 8C). These thin units of desiccated red mudstone rest on abrupt lacustrine flooding surfaces, indicating the continued presence of a fluctuating lake in the southeastern part of the study area (Fig. 8A) during deposition. The gradual fining-

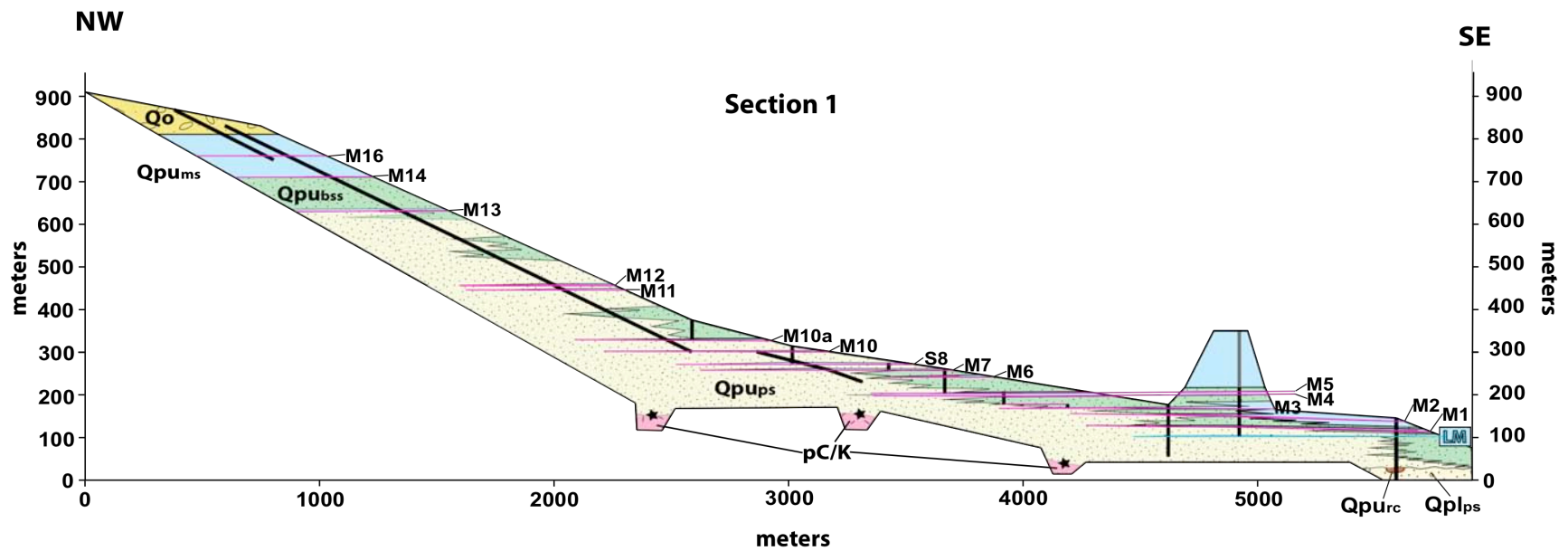


**Figure 9.** Facies panel for Section 1 showing northwest transgression of lacustrine mudstone and siltstone ( $Q_{pu_{ms}}$ ) and nearshore sandstone and siltstone ( $Q_{pu_{bss}}$ ) over distal alluvial fan pebbly sandstone ( $Q_{pu_{ps}}$ ) through time. Marker horizons shown as pink lines; LM is limestone marker horizon. Stars represent calculated depth-to-basement projected into section from nearby sediment – basement contacts.

upward lacustrine sequence high in Section 1, located at the northwest end of upper Painted Canyon (Fig. 4, Fig. 6A, Fig. 9), records a shift of the lacustrine depocenter to the northwest across a distance of ~ 4.5 km relative to the oldest lacustrine deposits near Eagle Canyon.

In upper Painted Canyon the Ocotillo Conglomerate conformably and gradationally overlies lake deposits at the top of the section, where it is truncated against the northeast side of the PCF and faulted down against the lower member of the Palm Spring Formation on the southwest side of the PCF (Fig. 4). In this area an anomalous, > 65-m thick coarsening upward wedge of Ocotillo Conglomerate close to the PCF thins laterally northeast into a typical ~ 25-m thick conglomerate over a map distance of ca. 300 m from the PCF.

#### ***Upper Member Northeast of the Painted Canyon Fault***

Sylvester & Smith (1976) noted the relatively thin nature of the upper Palm Spring member where it rests on intermittently exposed basement rock northeast of the PCF. Importantly, Section 1 (Fig. 6A) shows that despite relatively low bedding dips (< 14°) and shallow exposures of basement, the upper member is ~ 800 m thick northeast of the PCF. The relationship between basement and overlying deposits (Fig. 10) requires low-angle onlapping of the upper member onto basement (Fig. 8D) in order to reconcile the large measured thickness and shallow depth to basement in this area. While the mechanism that produced accommodation space for the ~ 800 m of deposits on shallow basement remains unclear, it is likely related to syn-depositional gentle tilting and translation of deposits out of a depocenter that was fixed relative to a releasing bend in the PCF, similar to the Ridge Basin in central California (e.g. Crowell, 2003).

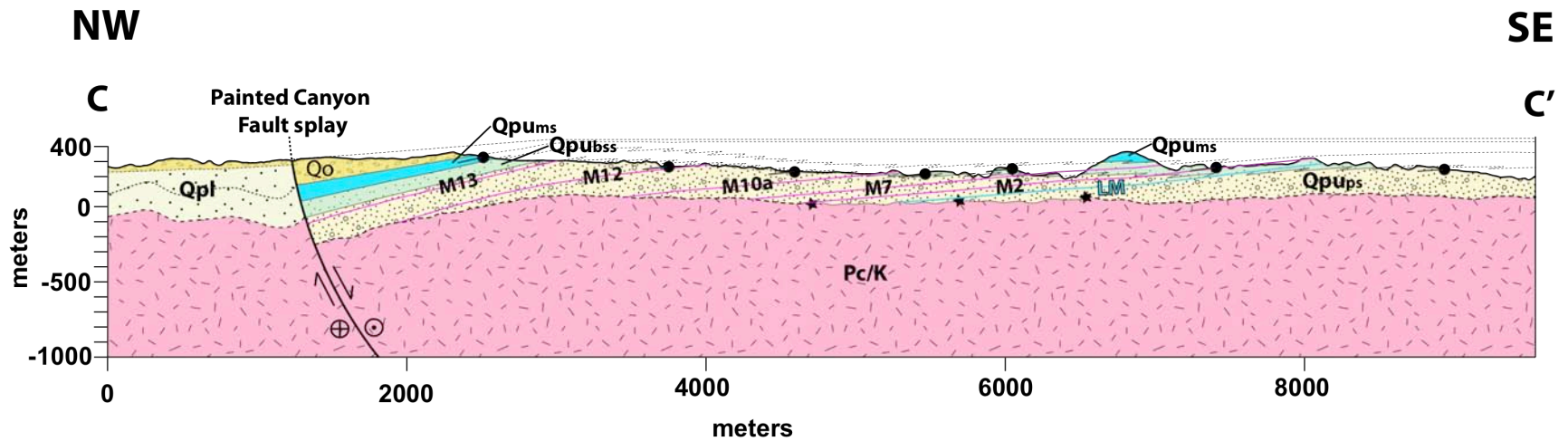


**Figure 10.** Geologic cross section line C – C' in Figure 4 on the northeast side of the PCF. Marker horizons used to correlate measured section 1 shown as pink lines and labeled (e.g. M2). LM is limestone marker horizon. Stars are calculated depth to basement projected into section from nearby basement exposures. Bedding dips and shallow basement requires low-angle down-lapping relationship of sedimentary rocks onto basement. Wedging of Ocotillo Conglomerate against transtensional Painted Canyon fault splay shown.

### ***Progressive Unconformity Southwest of the Painted Canyon Fault***

The contact between the lower and upper members of the Palm Spring Formation is a widespread angular unconformity that varies from high- to low-angle. Detailed mapping shows that the angular unconformity is discontinuous and time-transgressive in the area of lower Painted Canyon. The contact changes along strike from an angular unconformity near the southwest entrance of Box Canyon (Fig. 8E) to a laterally equivalent conformable surface at Painted Canyon, in the upper part of the lower Palm Spring member (~553 m in Section 3; Figs. 6B, 11). This surface is 117 m stratigraphically below a horizon that we mapped northwest along strike into a second, younger angular unconformity at the lower-upper Palm Spring contact northwest of Painted Canyon (Figs. 6B, 11).

The laterally discontinuous and time-transgressive nature of the angular unconformity is supported by mapping of the marker limestone bed (LM), which lies stratigraphically between the two unconformities (or laterally equivalent surfaces) in the area between lower Painted Canyon and Box Canyon (Fig. 11). This relationship suggests that (1) there are at least two distinct angular unconformities separating the lower and upper Palm Spring, and (2) the lower and upper members are laterally equivalent to each other in the interval between the two unconformities between Box Canyon and lower Painted Canyon (Figs. 11; 12). Estimates of stratigraphic thickness based on bedding attitudes and map distance indicate that the stratigraphic interval between the two unconformities thickens from ~117 m at Painted Canyon to ~230 m at a location 2.25 km southeast of lower Painted Canyon (Figs. 11; 12). This geometry provides evidence for sedimentation during intrabasinal deformation that produced the angular unconformity.

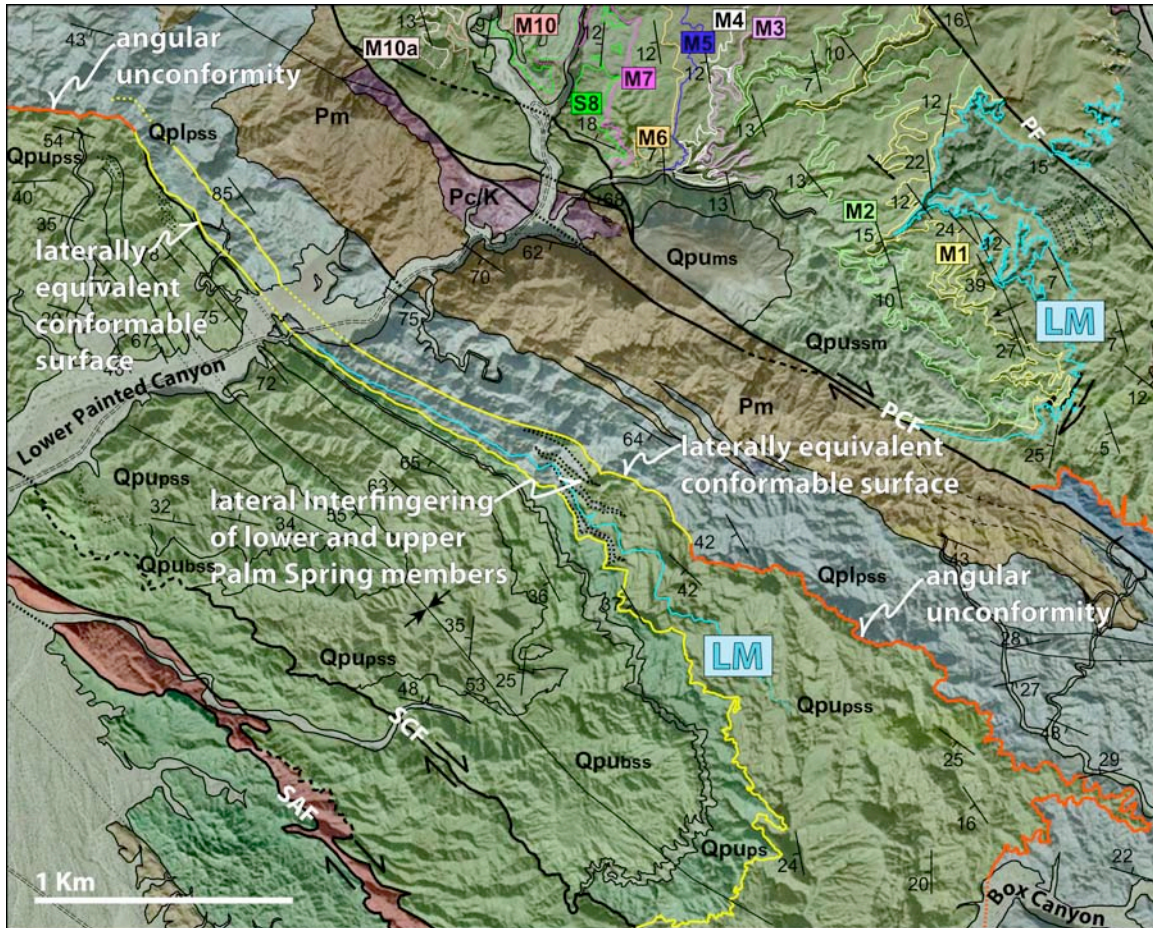


**Figure 11.** Map showing two angular unconformities (red lines), one in the northwest and one in the southeast, that separate the lower and upper members of the Palm Spring Formation. Both map into laterally equivalent conformable surfaces (yellow lines). Between the unconformities is an intermediate sedimentary package consisting of a southeast-thickening wedge of laterally interfingering lower and upper members of the Palm Spring Formation. Limestone unit LM maps within the intermediate package. Marker horizons used to correlate through Section 1 are shown northeast of the PCF.

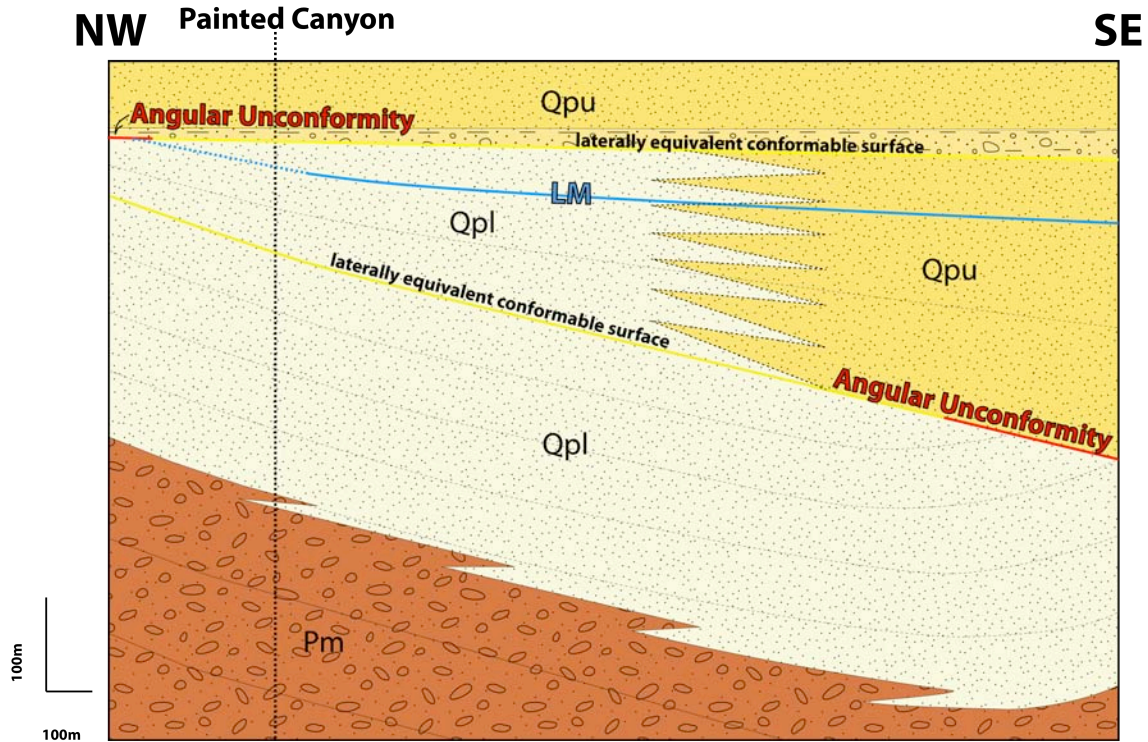


**Figure 12.** Simplified diagram illustrating the stratigraphic relationships in Figure 11 from northwest to southeast across Painted Canyon. Prominent lower unconformity in the southeast maps into a laterally equivalent conformable surface in the northwest. Upper unconformity in northwest maps into a laterally equivalent conformable surface in southeast. Intermediate southeast-thickening growth wedge of laterally interfingered lower and upper Palm Spring formation between unconformities. Limestone bed LM is within intermediate growth wedge.

## Stratigraphic Ages and Sediment-Accumulation Rates

### *Measured Section 1*

Our paleomagnetic sampling of Section 1 includes 50 sites that yielded 7 magnetic reversals and 8 magnetochrons. The Bishop Ash high in the section (exact stratigraphic position uncertain, projected into Section 1. Fig. 6A), located and identified northeast of the PCF by Michael Rymer (pers. communication, 2012) and confirmed in this study (Fig. 4), is an important marker that allows us to identify the normal-polarity Brunhes subchron (780 ka to present). A reversed-polarity site at 820 m in Section 1

suggests that the 780-ka reversal between the Brunhes and the underlying Matuyama magnetochron is located above 820 m and below the Bishop Ash, which we estimate to be between ~840 and ~870 m in Section 1 (Fig. 6A). Below this level, Section 1 contains most of the reversed-polarity Matuyama magnetochron including the normal-polarity Jaramillo, Olduvai, and Reunion subchrons (Fig. 6A). Using the minimum and maximum possible stratigraphic positions of reversals in Section 1, and their ages, we calculate minimum and maximum sediment accumulation rates for each magnetochron (Table 2). We extrapolate these accumulation rates to infer the ages of the major stratigraphic units and contacts between them. The age of the distinctive limestone marker horizon (LM) is thus estimated to be ~2.5 Ma with an uncertainty of 0.2 Ma, and the angular unconformity between the lower and upper members of the Palm Spring Formation is ~2.8 with an uncertainty of 0.3 Ma (Fig. 6A).

### ***Measured Section 3***

Paleomagnetic data from our sampling of Section 3 is problematic because it suggests only one reversal at the base of a thick section. Of the 58 sites sampled through ~1270 m of section, all but one site at the base of the section yielded negative polarity. We would expect Section 3 to contain some of the reversals recorded in Section 1 because of its great stratigraphic thickness and presence of the ca. 2.5-Ma LM limestone that is correlated from Section 1 (Fig. 6). This suggests at least two possible interpretations of the data and age of deposits in section 3, which we have constructed as two scenarios below.

**Table 2.** Calculated sediment-accumulation rates based on magnetic reversal ages and stratigraphic thickness from Section 1

Stratigraphic Interval	Time Interval (Ma)	Duration of Interval (k.y.)	Minimum Interval Thickness (m)	Maximum Interval Thickness (m)	Minimum Sedimentation Rate (mm yr <sup>-1</sup> )	Maximum Sedimentation Rate (mm yr <sup>-1</sup> )	Uncertainty (mm yr <sup>-1</sup> )
Bishop Ash* to Base of Brunhes	0.76-0.78	20,000	0	55	0	2.8	1.4
Base of Brunhes to top of Jaramillo	0.78-0.99	210,000	133	211	0.6	1.0	0.2
Top of Jaramillo to base of Jaramillo	0.99-1.07	80,000	55	96	0.7	1.2	0.3
Base of Jaramillo to top of Olduvai	1.07-1.79	720,000	194	236	0.3	0.3	0.1
Top of Olduvai to base of Olduvai	1.79-1.94	150,000	42	87	0.3	0.6	0.2
Base of Olduvai to top of Reunion	1.94-2.13	190,000	47	102	0.3	0.5	0.1
Top of Reunion to base of Reunion	2.13-2.15	20,000	3	51	0.2	2.6	1.2

\*Bishop Ash projected into measured section 1. Stratigraphic position unknown

*Scenario 1:* If we assume that the magnetic reversal between 2 and 19 m near the base of Section 3 (Fig. 6A) represents the boundary between the Gauss and Matuyama magnetochrons (2.58 Ma), we can calculate the predicted sediment-accumulation rates from this reversal to limestone unit LM. LM is found at 635 m in Section 3 and its age is estimated from section 1 between 2.3 Ma and 2.7 Ma. The measured thickness from the possible Gauss-Matuyama reversal to the limestone is thus ~ 615-633 m. The large uncertainty in our age estimates results in significant overlap of the age of the limestone unit and the Gauss – Matuyama boundary. The resulting sediment-accumulation rate for the ~620 m of section ranges from instantaneous deposition (geologically impossible) to ~6 mm/yr. This wide range of possible sediment-accumulation rates precludes well-constrained age estimates for stratigraphic boundaries in Section 3. Based on these assumptions a minimum sediment-accumulation rate of ~0.7 mm/yr, which is not included in our estimate range, is required to deposit the section from our reversal (at ~19 m) to the top of the section (at 1300 m) within the dominantly reverse-polarity Matuyama and explain the dominance of reverse-polarity sites in Section 3.

*Scenario 2:* Alternatively, the dominance of magnetically reversed sites in Section 3 may be due to reversed overprinting of some sites during the later part of the Matuyama magnetochron. In this case we could estimate sediment ages and accumulation rate in two ways: (1) use a range of sedimentation rates estimated for Section 1 (0.3 – 0.9 mm/yr) and extrapolate them from horizon LM; or (2) assume that the unconformity in Section 1 (~2.8 Ma, Fig. 6A) correlates to the lower unconformity in Section 3 (550 m, Fig. 6B), and calculate a sediment-accumulation rate between it and horizon LM in Section 3. Using assumption (1), we would estimate an age range of ~3.0-4.8 Ma for the base of the

Mecca Conglomerate, ~2.6-3.7 Ma for the base of the lower Palm Spring member, ~2.4-3.0 Ma for the lower unconformity, ~2.2-2.7 Ma for the upper unconformity (base of the upper Palm Spring member), and ~0.5-2.0 Ma for the top of the section. Using assumption (2) the sediment-accumulation rate would range from geologically impossible instantaneous deposition to ~0.1 mm/yr. The large uncertainty precludes useful age estimates under assumption (2).

Given the uncertainty in our age estimates, we tentatively use age ranges from Scenario 2, assumption (1), with the expectation that these estimates will change pending future sampling and analysis. Stratigraphic age estimates reported below carry uncertainties of ~0.3 – 1.0 Myr.

## CHAPTER V

### DISCUSSION

#### **Paleogeographic and Fault Reconstructions**

The data presented above allow us to reconstruct the paleogeography of the central Mecca Hills by tracking migration of depocenters and structurally controlled sub-basins through time (Fig. 13). In this section we interpret a ~ 4-Myr history of subsidence, deposition, and uplift along the southern San Andreas fault in this area based on the preceding stratigraphic analysis.

#### ***Mecca Conglomerate***

Prior to deposition of the Mecca Conglomerate, the central block was not accumulating sediment and basement rock likely was exposed and eroding at the surface. Beginning at roughly 3.0-4.8 Ma, subsidence of the Central Block lead to deposition of the Mecca Conglomerate in southwest-directed alluvial fans sourced from uplifted basement of the Platform Block (Fig. 13A). The presence of thick Mecca Conglomerate southwest of the PCF and its absence northeast of the fault suggests that southwest-side down slip on the PCF lead to subsidence of the Central Block and uplift of the Platform Block (Fig. 14A). Systematic fining-up in the upper Mecca Conglomerate records a transition to much more widespread subsidence and retrogradation of fluvial environments over fault-bounded alluvial fans prior to deposition. Retreat and submergence of alluvial fans likely was controlled by cessation of slip on the PCF, and either a decrease in the rate of sediment delivery or an increase in subsidence rate, or possibly both (e.g., Heller & Paola, 1992; Paola et al., 1992; Gordon & Heller, 1993).

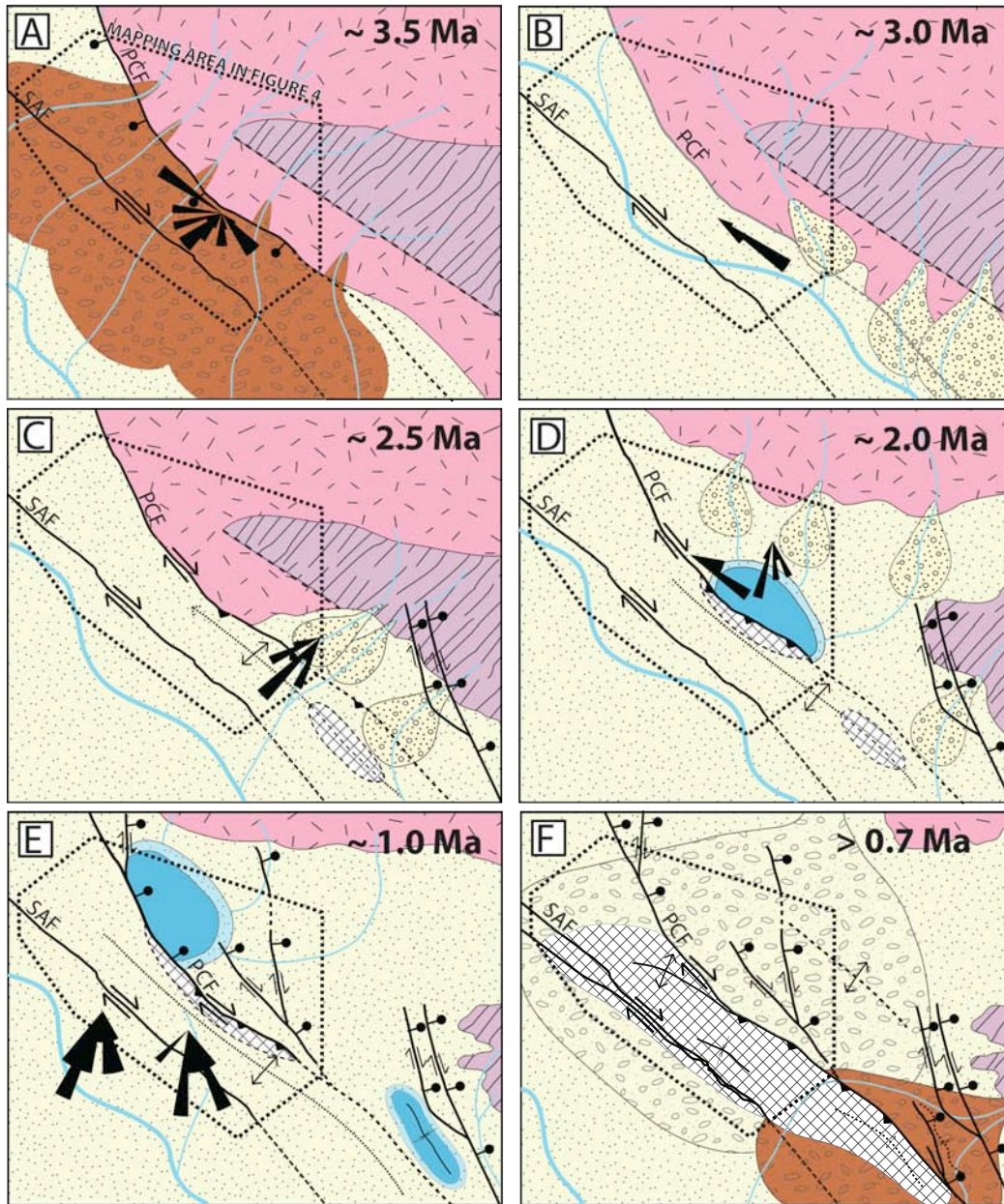


**Figure 13.** Paleogeographic reconstructions of the Mecca Hills from ~3.5 – 0.74 Ma. (A) Initiation of southwest-side down slip on the PCF and deposition of the Mecca Conglomerate between ~3.0-4.8Ma (B) Between 2.6 and 3.7 Ma the southeast-directed fluvial system deposited the lower member of the Palm Spring Formation across the alluvial fans of the Mecca Conglomerate and the PCF. (C) At roughly 2.4-3.0 Ma southwest-side up slip on the PCF resulted in deformation of the basin. (D) By ~2.4 Ma a lake system was established northeast of the PCF due to pooling of water against a topographic high along the PCF. (E) At ~1.0 Ma initiation of the transtensive PCF splay shifted the lake depocenter to the northwest. (F) post-700-ka uplift and erosion of the Mecca Hills shortly after deposition of the Ocotillo Conglomerate from progradation of gravel from the Cottonwood and Orocopia mountains.

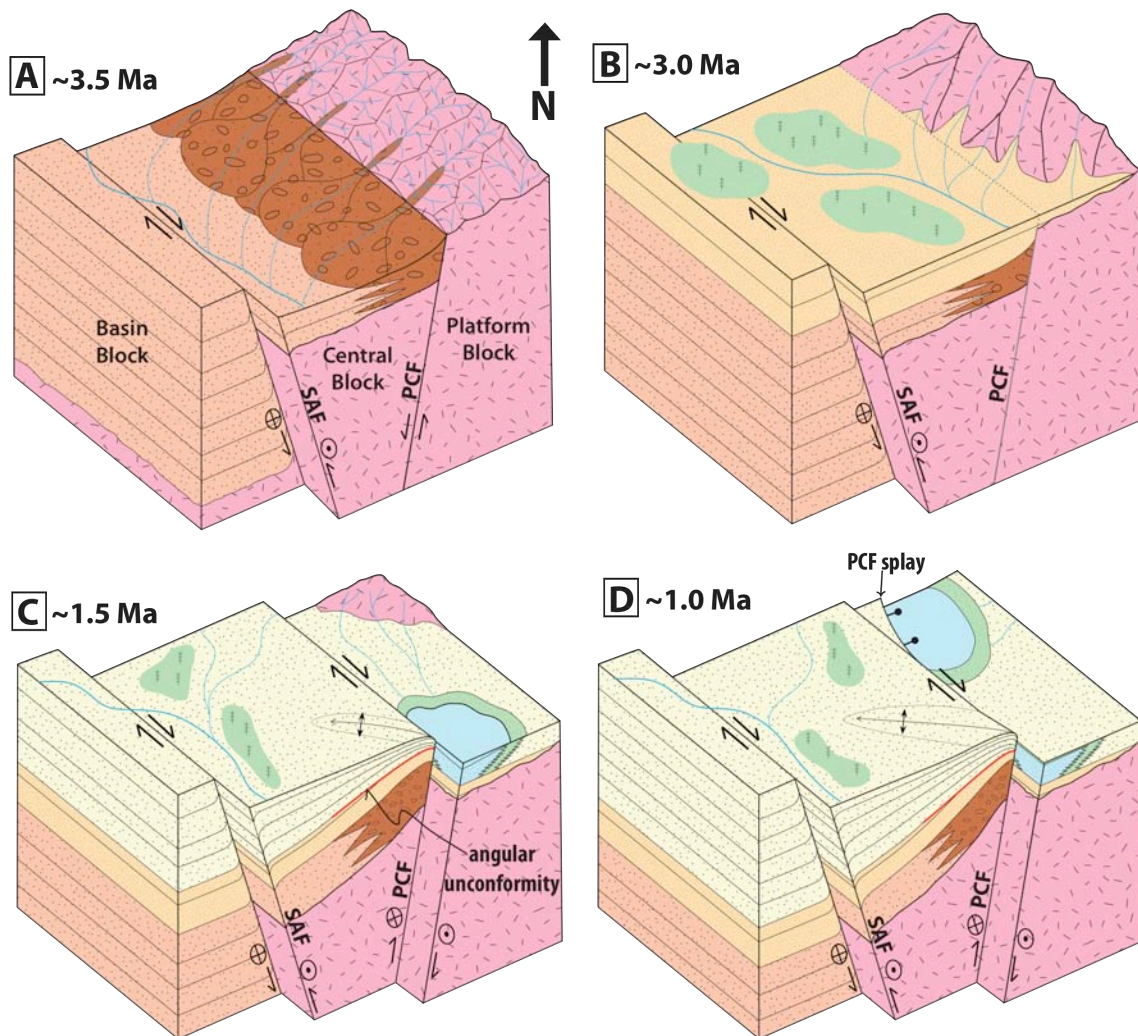


**Figure 14.** Block diagrams illustrating the evolution of vertical crustal motions and depositional systems from ~3.5 – 1 Ma in the Mecca Hills. (A) Southwest-side down slip on the PCF and deposition of the Mecca Conglomerate. (B) Overlapping deposition of the regionally extensive facies of the lower member of the Palm Spring Formation on the vertically quiescent PCF. Local conglomerates sourced from nearby basement highlands. (C) Southwest-side up slip of the PCF created the angular unconformity between the lower and upper members of the Palm Spring Formation, partitioned the basin along the PCF, and created a lake system northeast of the PCF (D) Initiation of the transpressive PCF splay shifted the lake depocenter to the northwest.

### ***Lower Member, Palm Spring Formation***

The lower member of the Palm Spring Formation was deposited across the PCF in a southeast-directed fluvial system beginning roughly 2.6-3.7 Ma (Fig. 13B). Similarity of facies in the lower member across the PCF, and lack of evidence for syntectonic deposition (unconformities, growth strata, etc.), suggests that subsidence and sedimentation were continuous over a large area during deposition (Figs 13B, 14B). The tabular sheet-like architecture of alternating sandstone and siltstone units suggests that the lower member accumulated in a broad river valley with dimensions similar to those of the modern Coachella Valley (Fig. 1).

### ***Deformation, Erosion, Angular Unconformity***

The angular unconformity between the lower and upper members of the Palm Spring Formation records the onset of localized deformation and a major structural reorganization of the fault zone at approximately 2.4-3 Ma (Fig. 13C). Southwest of the PCF, lateral interfingering of the lower and upper Palm Spring members, southeastward thickening of the upper member, and time-transgressive nature of the unconformity suggest that deposition continued at least locally in this area during deformation that created the unconformity (Fig. 12). This phase of deformation partitioned the basin into northeast and southwest sub-basins separated by the PCF, with each sub-basin accumulating distinct localized deposits (Figs 13D, 14C). In addition to localized deformation, regional subsidence and production of accommodation space is also required to explain continued deposition of the upper Palm Spring member throughout the Mecca Hills.

### *Upper Member, Palm Spring Formation*

The upper Palm Spring member records a change to more localized fault-controlled sedimentation and southwest-side up vertical displacement across the PCF while regional subsidence and production of accommodation space allowed for continued deposition throughout the Mecca Hills. Northeast of and adjacent to the PCF, a lake formed near Eagle Canyon shortly after deposition of the Palm Spring member began at ca. 2.8 Ma (Figs. 13D, 14C). We infer that water sourced from local rivers in the Cottonwood Mountains pooled on the northeast side of a topographic and structural high along the PCF. Evidence supporting this topographic high is seen in the presence of lower Palm Spring member clasts in upper the upper member (Fig. 7D) and growth strata within the upper member on the northeast side of the PCF (Fig. 8F). Southeast-directed alluvial fans sourced from the Cottonwood Mountains interacted at their lower end with the lake on the northeast side of the PCF. During deposition of the upper member at about 1.0 Ma, the lacustrine depocenter migrated ~ 4.5 km northwest due to localized subsidence northeast of a transtensional splay of the PCF (Figs. 13E, 14D). The lake remained fixed at this location until it was filled by deposition of the overlying Ocotillo Conglomerate.

Southwest of the PCF, deposition of the upper Palm Spring member persisted intermittently through deformation that created two angular unconformities (Fig. 12). After formation of the upper unconformity at roughly 2.2-2.5 Ma, it is unclear whether deposition took place on the flank of growing topography, or passively buried a submerged area of former uplift southwest of the PCF.

### ***Ocotillo Conglomerate (ca. 0.76 Ma)***

Significant slowing of subsidence shortly before 0.76 Ma resulted in basinward progradation of large alluvial fans from the Cottonwood and Orocopia mountains and deposition of the Ocotillo Conglomerate across most or all of the Mecca Hills (Fig. 13F). Northeast of the PCF, the Bishop Ash is interbedded in the lower part of the Ocotillo Conglomerate (Figs. 4, 6A), while southwest of the PCF the Bishop and Thermal Canyon ash are interbedded in the uppermost upper member of the Palm Spring Formation beneath the Ocotillo gravel (Fig. 4). This relationship shows that progradation of Ocotillo gravel took place around 760 ka, and supports geomorphic evidence that the gravel was derived from the Cottonwood and Orocopia mountains northeast of the Mecca Hills (fig. 13F). Thickening of Ocotillo Conglomerate in a localized wedge adjacent to the PCF in upper Painted Canyon records continued subsidence northeast of the northwestern PCF splay during gravel progradation (Fig. 13F). Ocotillo progradation likely was driven by slowing of regional subsidence during the transition from regional subsidence and sediment accumulation to the modern phase of uplift and erosion.

### **Local Versus Regional Scale of Fault-Zone Evolution**

It is well documented that local transpression and transtension within strike-slip fault zones results in significant rapid short-lived vertical displacements (e.g. Christie-Blick & Biddle, 1985; Teyssier et al., 1995; Aksu et al., 2000; Wakabayashi et al., 2004; Mann, 2007). Sinuous or anastomosing strike-slip fault zones are expected to produce localized migrating zones of transpressive and transtensive deformation due to the kinematics of translating rocks along non-linear fault surfaces (e.g. Christie-Blick & Biddle, 1985; Spotila et al. 1998; Wakabayashi et al. 2004; Cormier et al., 2006;

Benowitz et al., 2011). This can result in rapid local accumulations of sediments that are subsequently uplifted and eroded as they are translated through a heterogeneous strain field (e.g., Crowell, 1974; Saddler et al., 1993; Crowell, 2003). Therefore the spatial and temporal extent of deposits produced by deformation in strike-slip fault zones is governed to large degree by the spatial scale of local fault zone complexities and rates of fault slip.

In the Mecca Hills, evolution of local structures and the resulting complexly evolving strain field can explain the abundant nonlinear faults, complex history of fault-controlled deposition, reactivation and inversion of the PCF, migration of depocenters, and the time-transgressive angular unconformity. This explanation does not require any changes in relative plate motion or regional fault kinematics. According to this conceptual model, all deformation recorded in the stratigraphy of the Mecca Hills would be expected to occur at a spatial scale similar to that of local faults and fault-bounded blocks. Similarly, any stratigraphic signals produced by regional-scale tectonic changes should be expressed at a spatial scale significantly larger than that of local fault-zone complexities.

While much of the sedimentation and deformation history in the Mecca Hills can be explained by evolution of local fault-zone complexities, two prominent stratigraphic signals are recognized over a much larger area of the Coachella Valley and require a regional explanation. First, the angular unconformity separating the lower and upper members of the Palm Spring Formation is present along ~50 km of the SAF from the southeast Mecca Hills to the Indio Hills (Boley et al., 1994). This observation suggests that the episode of deformation that created the angular unconformity in the Mecca Hills reflects regional-scale adjustments along the southern SAF, and that deposition of the

upper Palm Spring member resulted from a return to regional-scale subsidence within a more complex and heterogeneous strain field. The age of the unconformity is not well dated in the Indio Hills, and thus the age correlation inferred here has yet to be fully tested.

Second, Late Cenozoic deposits that contain the Bishop Ash (760 ka) and Thermal Canyon Ash (740 ka) are currently being uplifted in a roughly 90 km long by 2-7 km wide belt adjacent to the Coachella Valley strand of the SAF, from Durmid Hill in the southeast to the northern Indio Hills in the northeast (Fig. 1). Bilham & Williams (1985) described the modern SAF in Coachella Valley as having a 'sawtooth' geometry with local deviations in fault strike that produce segmented areas of transpressive uplift in the Indio Hills, Mecca Hills, and Durmid Hill (Fig. 1). Prior to 740 ka, variable localized deformation along the SAF in Coachella Valley was superimposed on overall regional subsidence and sedimentation. It appears that a profound change in the regional behavior of the SAF in Coachella Valley has inverted a belt along the fault zone from net subsidence to net uplift and erosion that started at roughly 700 ka. The scale over which this inversion has occurred is much larger than the scale of local fault-zone complexities in the Mecca Hills. This tectonic event may be recorded in other areas of the southern SAF system, as seen in the onset of contractional deformation in the southern San Jacinto Fault zone at ca. 0.6 Ma (Steely et al. 2006; Lutz et al. 2006; Kirby et al. 2007), and the onset of rapid uplift and exhumation of fault-bounded crustal slices along the SAF in San Geronimo Pass at ca. 0.7 Ma (Spotila, 1998). The regional scale of post-700 ka basin inversion suggests that this change was driven by a regional rather than local control on the sense and distribution of vertical crustal motions along the fault zone.

Changes in the regional kinematics of the southern SAF zone may be linked to major reorganizations of the system through time. Initiation of the San Jacinto Fault zone ca. 1.2 Ma (e.g. Lutz et al., 2006; Steely et al. 2006; Janecke et al, 2010) apparently did not coincide with a significant change in the Coachella Valley segment of the southern SAF. Instead, the two regional tectonic reorganizations may be related to (1) changes in partitioning of slip rates between the San Jacinto fault and SAF through time (Bennett et al., 2004); or (2) trade-offs between slip focused on the SAF through San Geronio Pass versus transfer of strain northward through the Eastern Transverse Ranges into the Eastern California Shear zone (e.g., Dolan et al., 2007). The ultimate causes of regional changes in fault zone behavior and basin evolution along the southern SAF are not known and are the topic of ongoing study.

## CHAPTER VI

### CONCLUSIONS

Our stratigraphic analysis reveals a 3-4 Myr history of complex basin development and deformation along the Mecca Hills segment of the southern SAF. The tectonostratigraphic framework preserved in the Mecca Hills suggests that the paleo-landscape changed dramatically in response to rapid, punctuated, alternating periods of vertical displacements related to changing sense and patterns of slip on the PCF. The PCF changed from southwest-side down slip (Mecca Conglomerate) to vertically quiescent (lower member of Palm Spring Formation) to southwest-side up slip (upper Palm Spring member to the present), possibly with an increased rate of vertical offset after ~700 ka.

While the underlying controls on changes in kinematics of the PCF remain unclear, we conclude that basin evolution in the Mecca Hills was controlled by evolution of local fault-zone complexities superimposed on larger-scale changes in regional subsidence and uplift. Changes in regional fault kinematics likely caused extensive uplift and erosion along the SAF in Coachella valley at approximately 2.5-3 Ma, as recorded in a regional unconformity in the Mecca and Indio Hills, and again from ~0.7 Ma to the present as indicated by the current phase of regional uplift along the fault zone. Regional scale tectonic changes in this region are not well understood, but probably are related to alternation of slip transfer between the SAF, San Jacinto fault zone, and Eastern California shear zone.

Large uncertainties presently exist in our age estimates for deposits in the Mecca Hills that we hope to reduce with future paleomagnetic sampling and analysis. Improved

age constraints will allow for more precise evaluation of the timing, rates, and controls on basin evolution and deformation. This will provide improved insights into the relative importance of evolving fault-zone complexities versus changes in regional fault kinematics on basin development and deformation along the Coachella Valley segment of the southern SAF.

## REFERENCES CITED

- Aksu, A. E., T. J. Calon, R. N. Hiscott, and D. Yasar, 2000, Anatomy of the North Anatolian Fault zone in the Marmara sea, western Turkey: Extensional basins above a continental transform, *GSA Today*, v. 10, p. 3–7.
- Atwater, T., 1970, Implications of plate tectonics on the Cenozoic tectonic evolution of Western North America, *Geol. Soc. Am. Bull.*, v. 81, p. 3513-3536.
- Axen, G.J., and Fletcher, J.M., 1998, Late Miocene-Pleistocene extensional faulting, Northern Gulf of California, Mexico and Salton Trough, California. *International Geology Review*, v. 40, p. 217-244.
- Behr, W.M., Rood, D.H., Fletcher, K.E., Guzman, N.E., Finkel, R., Hanks, T.C., Hudnut, K.W., Kendrick, K.J., Platt, J.P., Sharp, W.D., Weldon, R.J., and Yule, J.D., 2010, Uncertainties in slip rate estimates for the Mission Creek strand of the southern San Andreas fault at Biskra Palms oasis: Southern California: *Geological Society of America Bulletin*, v. 122, p. 1360–1377.
- Bennett, R. A. Friedrich, A. M., and Furlong, K. P., 2004, Codependent histories of the San Andreas and San Jacinto fault zones from inversion of fault displacement rates: *Geology*, v. 32, p. 961-964.
- Benowitz, J.A., Layer, P.W., Armstrong, P, Perry, S.E., Haeussler, P.J., Fitzgerald, P.G., and VanLaningham, S., 2011, Spatial variations in focused exhumation along a continental-scale strike-slip fault: The Denali fault of the eastern Alaska Range. *Geosphere*, v. 7, p. 455–467.
- Blair, T.C., 1987a, Sedimentary processes, vertical stratification sequences, and geomorphology of the Roaring River alluvial fan, Rocky Mountain National Park, Colorado. *Journal of Sedimentary Petrology* v. 57, p. 1–18.
- Blair, T.C. and McPherson, J.G., 1994, Alluvial fans and their natural distinction from rivers based on morphology, hydraulic processes, sedimentary processes, and facies assemblages. *J. Sed. Res.*, v. 64, p. 450–489.
- Boley, J.L., 1993, Block rotation and magnetostratigraphy along the southern San Andreas fault zone, California [MS. thesis]: University of Oregon, 200 pp.
- Boley, J.L., Stimac, J.P., Weldon, R.J., and Rymer, M.J., 1994, Stratigraphy and paleomagnetism of the Mecca and Indio Hills, southern California. In: McGill, S.F., and Ross, T.M., eds., *Geological Investigations of an Active Margin: Geological Society of America, Cordilleran Section Guidebook, Trip 15*, p. 336-344.

- Burgmann, R., 1991, Transpression along the southern San Andreas fault, Durmid Hill, California. *Tectonics*, v. 10, p. 1152-1163.
- Chang, S-B.R., Allen, C.R., and Kirschvink, J.L., 1987, Magnetic stratigraphy and a test for block rotation of sedimentary rocks within the San Andreas fault zone, Mecca Hills, southeastern California. *Quaternary Research*, v. 27, p. 30-40.
- Christie-Blick, N., and Biddle, K.T., 1985, Deformation and basin formation along strike-slip faults, in Biddle, K.T., and Christie-Blick, N., eds., *Strike-slip deformation, basin formation, and sedimentation*. SEPM Special Publication 37, p. 1-34.
- Cormier, M.H., Seeber, L., McHugh, C.M.G., Polonia, A., Cagatay, M.N., Emre, O., Gasperini, L., Gorur, N., Bertoluzzi, G., Bonatti, E., Ryan, W.B.F., and Newman, K.R., 2006, The North Anatolian fault in the Gulf of Izmit (Turkey): Rapid vertical motion in response to minor bends of a non-vertical continental transform: *Journal of Geophysical Research*, v. 111, B04102, doi: 0.1029/2005JB003633.
- Crowell, J.C., 1974, Origin of late Cenozoic basins in southern California, in Dickinson, W.R. (ed.), *Tectonics and Sedimentation*. SEPM Special Publication 22, p. 190-204.
- Crowell, J.C., ed., 2003, *Evolution of Ridge Basin, Southern California: An Interplay of Sedimentation and Tectonics*: Geological Society of America Special Paper, p. 367, 247
- Dibblee, T. W., Jr., 1954, Geology of the Imperial Valley region, California. *Geology of Southern California*, California Division of Mines Bulletin v. 170, p. 21-28.
- Dibblee, T.W., 1997. Geology of the southeastern San Andreas fault zone in the Coachella Valley area, southern California. In: Baldwin et al. (eds.) *Southern San Andreas fault –Whitewater to Bombay Beach, Salton Trough, California*. South Coast Geological Society, Field Trip Guidebook No. 25, p. 35-56.
- Dolan, J.F., Bowman, D.D., and Sammis, C.G., 2007, Long-range and long-term fault interactions in southern California: *Geology*, v. 35, no. 9, p. 855–858, doi: 10.1130/G23789A.1.
- Dorsey, R.J., 2010, Sedimentation and crustal recycling along an active oblique-rift margin: Salton Trough and northern Gulf of California. *Geology*, v.38, p. 443-446.
- Dorsey, R.J., Housen, B.A., Janecke, S.U., Fanning, C.M., and Spears, A.L.F., 2011, Stratigraphic record of basin development within the San Andreas fault system: Late Cenozoic Fish Creek-Vallecito basin, southern California. *Geological Society America Bulletin*, v. 123, p. 771-793.

- Dorsey, R.J., V.E. Langenheim, J.C. McNabb, 2012, Geometry, Timing, and Rates of Active Northeast Tilting Across the Southern Coachella Valley and Santa Rosa Mountains, Abstract T51B-2568 presented at 2012 Fall Meeting, AGU, San Francisco, Calif., Dec. 3-7
- Elders, W.A., R.W. Rex, T. Meidav, P.T. Robinson, and S. Biehler, 1972, Crustal spreading in Southern California: The Imperial Valley and the Gulf of California formed by rifting apart of a continental plate, *Science*. v. 178, p. 15-24.
- Elders, W.A. & Sass, J.H., 1988, The Salton Sea scientific drilling project. *Journal of Geophysical Research*, 93, Issue B11, p. 12,953-12,968.
- Fattaruso, L., M.L. Cooke, 2013, The influence of complex fault geometry on uplift patterns in the Coachella Valley and Mecca Hills of Southern California, Abstract T13D-2644. 2013 Fall Meeting, AGU, San Francisco, Calif., 9-14 Dec.
- Fuis, G.S., Mooney, W.D., Healy, J.H., McMechan, G.A. and Lutter, W.J., 1984, A seismic refraction survey of the Imperial Valley Region, California: *Journal of Geophysical Research*, v. 89, p. 1165-1189.
- Fuis, G. S., D. S. Scheirer, V. E. Langenheim, and M. D. Kohler, 2012, A new perspective on the geometry of the San Andreas fault in southern California and its relationship to lithospheric structure, *Bull. Seismol. Soc. Am.*, 102, 236–251, doi:10.1785/0120110041.
- Gordon, I., and Heller, P. L., 1993, Evaluating major controls on basinal stratigraphy, Pine Valley, Nevada: Implications for syntectonic deposition: *Geological Society of America Bulletin*, v. 105, no. 1, p. 47-55.
- Hampton, B.A., and Horton, B.K., 2007, Sheetflow fluvial processes in a rapidly subsiding basin, Altiplano plateau, Bolivia. *Sedimentology*, v. 54, p. 1121–1147.
- Heller L, Paola C, 1992, The large-scale dynamics of grain-size variations in alluvial basins 2. Application to syntectonic conglomerate. *Basin Res* v. 4, p. 91–102
- Ingersoll, R.V., and Rumelhart, P.E., 1999, Three-stage evolution of the Los Angeles basin, southern California: *Geology*, v. 27, p. 593–596, doi: 10.1130/0091-7613(1999)027<0593:TSEOTL>2.3.CO;2.
- Janecke, S.U., Dorsey, R.J., Steely, A.N., Kirby, S.M., Lutz, A.T., Housen, B.A., Belgarde, B., Langenheim, V., Rittenour, T., and Forand, D., 2010, High geologic slip rates since early Pleistocene initiation of the San Jacinto and San Felipe fault zones in the San Andreas fault system: Southern California, USA. *Geological Society of America Special Paper*, v. 48, p. 475

- Keller, E.A., Bonkowski, M.S., Korsch, R.J., and Shlemon, R.J., 1982, Tectonic geomorphology of the San Andreas fault zone in the Southern Indio Hills, Coachella Valley, California. *Geological Society of America Bulletin*, v. 93, p. 46–56.
- Kirby, S. M., S. U. Janecke, R. J. Dorsey, B. A. Housen, V. Langenheim, K. McDougall, and A. N. Steely, 2007, Pleistocene Brawley and Ocotillo formations: Evidence for initial strike-slip deformation along the San Felipe and San Jacinto fault zones, southern California, *J. Geol.*, v. 115, p. 43–62, doi:10.1086/509248.
- Langenheim, V.E., Jachens, R.C., Matti, J.C., Hauksson, E., and Christensen, A., 2005, Geophysical evidence for wedging in the San Gorgonio Pass structural knot, southern San Andreas fault zone, southern California. *GSA Bulletin*, v. 117; p. 1554–1572.
- Law, R.D., Eriksson, Kenneth, Davisson, Cole, 2001. Formation, evolution, and inversion of the middle Tertiary Diligencia basin, Orocochia Mountains, southern California. *GSA Bulletin* v. 113, p. 196–221.
- Lutz, A.T., Dorsey, R.J., Housen, B.A., and Janecke, S.U., 2006, Stratigraphic record of Pleistocene faulting and basin evolution in the Borrego Badlands, San Jacinto fault zone, southern California: *Geological Society of America Bulletin*, v. 118, p. 1377–1397, doi: 10.1130/B25946.1.
- Mann, P., 2007, Global catalogue, classification and tectonic origins of restraining and releasing bends on active and ancient strike- slip fault systems, in *Tectonics of Strike- Slip Restraining and Releasing Bends*, edited by W. D. Cunningham and P. Mann, *Geol. Soc. Spec. Publ.*, v. 290, p. 13–142.
- McDougall, K., Poore, R.Z., and Matti, J.C., 1999, Age and environment of the Imperial Formation near San Gorgonio Pass, California: *Journal of Foraminiferal Research*, v. 29, p. 4–25.
- Messe, G.T., J.C. McNabb, B.A. Housen, R.J. Dorsey, 2012, Magnetostratigraphy of the Palm Spring Formation, Mecca Hills, CA, *GSA Abstracts with Programs*, 44, xxx.
- Miall, A.D., 1985, Architectural element analysis: a new method of facies analysis applied to fluvial deposits. *Earth-Sci. Rev.*, v. 22, p. 261–308.
- Miller, D.D., 1998, Distributed shear, rotation, and partitioned strain along the San Andreas fault, central California. *Geology*, v. 26, p. 867–870.

- Morton, D.M., and Matti, J.C., 1993, Extension and Contraction Within an Evolving Divergent Strike-Slip Fault Complex: The San Andreas and San Jacinto Fault Zones at Their Convergence in Southern California. In Powell, R.E.; Weldon, R. J.; and Matti, J.C.; eds., *The San Andreas Fault System: Displacement, Palinspastic Reconstruction, and Geologic Evolution*. Geological Society of America, *Memoir v. 178*, p. 217-230.
- Mulder, T. and Alexander, J., 2001, The physical character of subaqueous sedimentary density flows and their deposits. *Sedimentology*, v. 48, p. 269–299.
- Nichols, G.J., Hirst, J.P.P., 1998, Alluvial fans and fluvial distributary systems, Oligo-Miocene, northern Spain: contrasting processes and products. *Journal of Sedimentary Research* v. 68, p. 879–889.
- Oskin, M., and Stock, J., 2003a, Marine incursion synchronous with plateboundary localization in the Gulf of California: *Geology*, v. 31, p. 23–26, doi: 10.1130/00917613(2003)031<0023:MISWPB>2.0.CO;2.
- Oskin, M., and Stock, J., 2003b, Pacific–North America plate motion and opening of the Upper Delfin basin, northern Gulf of California, Mexico: *Geological Society of America Bulletin*, v. 115, p. 1173–1190, doi: 10.1130/B25154.1.
- Paola C, Heller PL, Angevine CL, 1992, The large scale dynamics of grain-size variations in alluvial basins, 1. *Theory Basin Res* v. 4, p. 73–90
- Parsons, T., and J. McCarthy, 1996, Crustal and upper mantle velocity structure of the Salton Trough, southeast California, *Tectonics*, v. 15, p. 456–471.
- Sadler, P., Demirer, A., West, D., and Hillenbrand, J.M., 1993, The Mill Creek Basin, the Potato Sandstone, and fault strands in the San Andreas fault zone south of the San Bernardino Mountains. In: Powell, R. E., Weldon, R. J., and Matti, J. C. (Eds.), *The San Andreas Fault System: Displacement, Palinspastic Reconstruction, and Geologic Evolution*. *Geol. Soc. Am. Memoir*, v. 178, p. 289-306.
- Seeber, L., Cormier, M.-H., McHugh, C., Emre, Ö., Polonia, A., and Sorlien, C., 2006, Rapid subsidence and sedimentation from oblique slip near a bend on the North Anatolian Transform in the Marmara Sea, Turkey, *Geology*, v. 34, p. 933–936.
- Seeber, L., Sorlien, C., Steckler, M., and Cormier, M.H., 2010, Continental transform basins: Why are they asymmetric? *Eos*, Vol. 91, No. 4, p. 29-30.
- Sheridan, J.M., and Weldon, R.J. II, 1994, Accommodation of compression in the Mecca Hills, California, in *Geological Investigations of an Active Margin: Guidebook*, 1994, Geological Society of America, Cordilleran Section, S. F. McGill and T. M. Ross (Editors), San Bernardino County Museum, Redlands, California, p. 330–336.

- Shirvell, C. R., D. F. Stockli, G. J. Axen, and M. Grove, 2009, Miocene- Pliocene exhumation along the west Salton detachment fault, southern California, from (U Th)/He thermochronometry of apatite and zircon, *Tectonics*, v. 28, TC2006, doi:10.1029/2007TC002172.
- Sieh, K.E., and Williams, P.L., 1990, Behavior of the southernmost San Andreas fault during the past 330 years, *J. Geophys. Res.* v. 95, p. 6629–6645.
- Spotila, J.A., Farley, K.A., and Sieh, K., 1998, Uplift and erosion of the San Bernardino Mountains, associated with transpression along the San Andreas fault, CA, as constrained by radiogenic helium thermochronometry: *Tectonics*, v. 17, p. 360–378.
- Spotila, J.A., House, M.A., Niemi, N.A., Brady, R.C., Oskin, M., and Buscher, J.T., 2007a, Patterns of bedrock uplift along the San Andreas fault and implications for mechanisms of transpression, in Till, A.B., Roeske, S.M., Sample, J.C., and Foster, D.A., eds., *Exhumation Associated with Continental Strike-Slip Fault Systems: Geological Society of America Special Paper 434*, p. 15–33.
- Spotila, J.A., Niemi, N.A., Brady, R.C., House, M.A., Buscher, J.T., and Oskin, M., 2007b, Longterm continental deformation associated with transpressive plate motion: The San Andreas fault. *Geology*, v. 35, p. 967-970.
- Steely, A.N., Janecke, S.U., Dorsey, R.J. and Axen, G.J., 2009, Early Pleistocene initiation of the San Felipe fault zone, SW Salton Trough, during reorganization of the San Andreas fault system. *Geological Society of America Bulletin*, v. 121, p. 663-687.
- Stock, J.M., and Hodges, K.V., 1989, Pre-Pliocene extension around the Gulf of California and the transfer of Baja California to the Pacific Plate: *Tectonics*, v. 8, p. 99–115, doi: 10.1029/TC008i001p00099.
- Stock, J.M., and Hodges, K.V., 1989, Pre-Pliocene extension around the Gulf of California and the transfer of Baja California to the Pacific plate: *Tectonics*, v. 8, p. 99–115.
- Sylvester, A. G., and Smith, R.R., 1976, Tectonic transpression and basement-controlled deformation in San Andreas fault zone, Salton Trough, California, *Am. Assoc. Pet. Geol. Bull.*, v. 60, p. 2081-2102.
- Sylvester, A.G., 1999, Rifting, transpression, and neotectonics in the central Mecca Hills, Salton Trough. In: Cooper, J.D. (ed.) *Pacific Section SEPM Fall Field trip Guidebook*, Pacific Section SEPM Book 85, p. 1-11.
- Teyssier, C., Tikoff, B., and Markley, M., 1995, Oblique plate motion and continental tectonics. *Geology*, v. 23, p. 447-450.

- Wakabayashi, J., Hengesh, J.V., and Sawyer, T.L., 2004, Four-dimensional transform fault processes: Progressive evolution of stepovers and bends: *Tectonophysics*, v. 392, no. 1–4, p. 279–301.
- Weldon, R.J., Meisling, K.E., and Alexander, J., 1993, A speculative history of the San Andreas fault in the Transverse Ranges, California. In: Powell, R. E., Weldon, R. J., and Matti, J. C. (Eds.), *The San Andreas Fault System: Displacement, Palinspastic Reconstruction, and Geologic Evolution*. *Geol. Soc. Am. Memoir*, v. 178, p. 161-198.
- Wilcox, R.E., Harding, T.P., and Seely, R., 1973, Basic wrench tectonics, *Am. Assoc. Pet. Geol. Bull.*, v. 57, p. 74-96.
- Winker, C.D., 1987, Neogene stratigraphy of the Fish Creek–Vallecito section, southern California: Implications for early history of the northern Gulf of California and Colorado delta [Ph.D. thesis]: Tucson, University of Arizona, 494 p.
- Winker, C.D. and Kidwell, S.M., 1996, Stratigraphy of a marine rift basin: Neogene of the western Salton Trough, California, in Abbott, P.L., and Cooper, J.D., eds., *Field conference guidebook and volume for the AAPG annual convention*, p. 295-336